To the Graduate Council:

I am submitting herewith a thesis written by Marcia A. Kohls entitled "A Hybrid Fuzzy-Wavelet Approach to Medical Image Fusion." I have examined the final copy of this thesis for form and content and recommend that it be accepted in partial fulfillment of the requirements for the degree of Master of Science, with a major in Engineering Science.

Israel E. Alguíndigue, Major Professor

We have read this thesis
and recommend its acceptance:

Robert E. Uhrig

Accepted for the council:

Associate Vice Chancellor and
Dean of The Graduate School

A HYBRID FUZZY-WAVELET APPROACH

TO MEDICAL IMAGE FUSION

A Thesis

Presented for the

Master of Science

Degree

The University of Tennessee, Knoxville

Marcia Adriane Kohls

August 1997

To my parents, Adelmo Kohls and Cenilda Norma Kohls, whose dedication, sacrifice, and vision have been my encouragement throughout this journey, and my model in life.

To my brother, Airton Gustavo Kohls, my best roommate and greatest source of laughs and support for four great years.

ACKNOWLEDGEMENTS

I would first like to thank my advisor and great friend, Dr. Israel E. Alguíndigue. His support, technical advice, and insight have been invaluable throughout this research; his commitment, friendship, and enthusiasm a great inspiration during difficult times. I would also like to thank Dr. Robert E. Uhrig of the Nuclear Engineering Department, and Dr. Estéban Walker of the Statistics Department, for agreeing to participate as members of my thesis committee. Many thanks to Dr. Laurence F. Miller of the Nuclear Engineering Department and Dr. Stephanie Smullen of the Computer Science and Electrical Engineering Department at the University of Tennessee at Chattanooga for their contributions to the successful completion of this thesis.

I would like to express my gratitude to Dr. Gary Smith of the University of Tennessee Medical Center and to Dr. Luc Bidaut of the Geneva University Hospitals for providing me with some of the images used for the validation of this research work. I also wish to acknowledge another set of images obtained from the "Whole Brain Atlas", an information resource for central nervous system imaging at Harvard Medical School.

The ideas developed in this thesis would not exist without the vision of my dear friend Aucyone da Silva. His interest and devotion to the topic of wavelets made this research a reality, and I have no adequate words to describe my appreciation for the numerous hours he spent teaching and advising me on this subject. This thesis would not have been completed without his help and guidance.

Finally, my sincere thanks to all whom directly and indirectly contributed to the development of this research work with suggestions, encouragement, and friendship. My parents, brother, and family in Brasil have always been an incredible source of strength and inspiration. Jerry and Bernice Parker and family, my "American family", have supported and encouraged me for many years now, and I am extremely grateful for their friendship and guidance. Thank you Cenk, for brightening my life with your adventurous mind and spirit. My friends are also my family, specially since being away from Brasil for so many years. I would like to thank each and everyone of them for their uniqueness and presence in my life, specially the Brazilian, Turkish, Mexican, and Venezuelan communities, who have delighted me with their colors, songs, stories, and culture. Muito obrigado pessoal!! Tesekkürler!! Muchíssimas gracias!!

ABSTRACT

Much concern remains in the ability of physicians to provide a timely and accurate medical diagnosis. Tremendous efforts are made in the thorough analysis of images to extract, combine and visualize the most representative features within an image for the characterization of the respective pathological condition. The aim of this research work is to provide an alternative approach for effectively combining relevant anatomical and functional information from different scanning modalities in a fused output image.

For this work, preprocessed and coregistered Magnetic Resonance (MRI) images and Positron Emission Tomography (PET) scans are decomposed by a discrete wavelet transform (DWT) in successive resolution steps and represented by matrices of wavelet coefficients at the corresponding resolution levels. These MRI and PET coefficient matrices are then fused in a fuzzy inference system (FIS) to produce a single set of coefficient matrices which characterize both the PET and MRI features. The "fuzzy engine" implementation allows for a robust and flexible representation of the rules that determine the method of coefficient selection for the actual fusion of the wavelet coefficients. Finally, the resulting fused coefficient matrices are reconstructed by an inverse wavelet transform (IWT) in order to obtain the output fused image.

The fuzzy-wavelet system hereby proposed consists of a novel fusion technique by taking advantage of the superb spatial and frequency characterization of wavelets and of the robustness of the fuzzy inference system design. Coregistered sets of brain images are analyzed by using different wavelet basis functions and different FIS designs, and all resulting images demonstrate the effectiveness of the method. Best results are obtained by utilizing Daubechies and biorthogonal wavelets with lower vanishing moments; FIS designs may be optimized to enhance specific features from either PET or MRI input images at the physician's criteria. The output fused image may be further compressed by processing with the DWT for ease of storage.

TABLE OF CONTENTS

LIST OF FIGURES

CHAPTER 1

INTRODUCTION

1.1 Statement of the Problem

The medical community has both witnessed and helped to promote an incredible technological breakthrough in the medical imaging field in the past decade, with continuous improvements in the flexibility, power, and diagnostic utility of the different imaging modalities. As a result, more applications of such imaging devices are being explored in clinical and research environments, and more data is produced and made available for further analysis and evaluation.

In a hospital setting, where recently doctors only relied on radiographs for diagnostic purposes, a wealth of images from sophisticated scanners are readily produced to aid the physician in the visualization of the anatomy and function of a specific organ. These images are obtained from different imaging techniques and become the main support of clinical diagnosis, planning and evaluation of therapy, since they provide complimentary information. More specifically, Computed Tomography (CT), Magnetic Resonance Imaging (MRI), Ultrasound and X-rays provide great anatomical detail, but little functional information. On the other hand, Single Photon Emission Computed Tomography (SPECT), Positron Emission Tomography (PET), and Magnetic Resonance Spectroscopy (MRS) depict functional aspects very clearly, but poorly delineate anatomy.

As some of these sophisticated devices are more routinely utilized and become more cost efficient (specially MRI and PET), a need for a systematic analysis of a large volume of complementary images arises.

Many situations occur in which data from complementary types of medical studies from the same patient need to be correlated and combined for a complete evaluation of the pathological condition. In radiation therapy planning, a CT scan is used for dose distribution calculations, while the contours of the target lesion are often best outlined on MRI [1]. The determination of the anatomical location of dysfunctional areas in nuclear medicine is usually based on data from PET, SPECT, MRI and CT scans. Specific applications include the use of the above mentioned imaging modalities for the evaluation of Alzheimer's disease in the elderly and in younger HIV-positive patients with symptoms of dementia [2], the utilization of SPECT, CT, and MRI for evaluation of hemangiomas [2], as well as improving PET or SPECT reconstruction with anatomical information from MRI [1].

It is therefore obvious that the ability to combine relevant morphological and functional information from different scanning modalities in a fused output image emerges as a crucial alternative tool for an enhanced and faster medical diagnosis. The fused output image accurately depicts the functional-structural relationship of the data, provides a composite overview of the pathology being surveyed, and aids in the reduction of the volume of data to be simultaneously evaluated. The physician may at this stage focus on a single image portraying the spatial-functional characteristics of the region being evaluated without the burden of separately analyzing each modality of scan in order to establish the correspondence among them.

1.2 Proposed Solution and Significance of the Project

This project introduces and develops a new methodology for medical image fusion that utilizes and combines the wavelet based multiresolution analysis (MRA) method and the fuzzy logic technology. Wavelet transform applications excel in the biological and medical fields by being particularly suitable to the analysis of nonstationary signals [3]. Most biomedical signals do present complex time-frequency or spatial-frequency characteristics, and therefore need to be evaluated with a technique such as the wavelet transform which exhibits great frequency resolution combined with fine time and spatial characterization. Similarly, the abundance of fuzzy logic applications in areas such as image enhancement and scene analysis proves the effectiveness of the method in the modeling of conditions that are inherently imprecisely defined.

The images utilized in this research work comprise sets of MRI and PET scans of the head. Prior to their analysis and subsequent fusion with the fuzzy-wavelet method, the multimodality brain images may be preprocessed for background removal and noise reduction or for enhancement, which may consist of edge detection [4-5], image segmentation [6], and enhancement by various filtering methods [7], according to the nature of the specified images. Furthermore, a crucial requirement for fusion of images of disparate modalities is registration. It is absolutely imperative that the set of images be coregistered, that is, matched spatially to a very accurate level, in order to ensure proper alignment of features. While registration remains a rather complex task in any imaging system, it is not addressed in this research, but constitutes a major assumption of the proposed implementation.

The preprocessed and coregistered MRI and PET head images are decomposed by a discrete wavelet transform in successively lower resolution steps and are represented by matrices of wavelet coefficients at the corresponding resolution levels. These MRI and PET coefficient matrices are then fused in a fuzzy inference system to produce a single set of coefficient matrices which characterize both the PET and MRI features. It should be noted that one of the main advantages of the method proposed is precisely the notion of performing the fusion on the wavelet coefficients that represent the images rather than on the images themselves. The "fuzzy engine" implementation allows for a robust and flexible representation of the rules that determine the method of coefficient selection for the actual fusion of the wavelet coefficients. Finally, the resulting fused coefficient matrices are reconstructed by an inverse wavelet transform in order to obtain the output fused image.

The fuzzy-wavelet system hereby proposed consists of a novel fusion technique by taking advantage of the superb spatial and frequency characterization of wavelets and of the robustness of the fuzzy inference system design. By utilizing a wavelet transform in the proposed methodology, the system designer not only ensures the general compatibility of the method to the type of signal being evaluated (nonstationary two-dimensional signal), but also has the flexibility to determine which prototype function ("mother wavelet") best suits and describes the signal under consideration. Also, the inherent characteristics of features within each image are at no point modified by their processing, simply because any transformation or manipulation is performed locally on the wavelet coefficients at specific resolution levels, without compromising the overall structural integrity of the image. Furthermore, the decomposition of the image by the wavelet multiresolution approach allows for the elimination of redundant information contained at different resolution levels. This is accomplished by choosing to perform the reconstruction solely with the levels and matrices that carry the relevant characteristics desired in the fused output image. The introduction of the fuzzy inference system as the tool for the fusion of the chosen wavelet coefficient matrices grants more flexibility to the implementation by avoiding a very exact or "hard" definition of the rules that determine the combination of the inherent "fuzzy" PET data and the more precise MRI data.

The primary goal of this research is therefore to investigate the application of the proposed hybrid fuzzy-wavelet method to the fusion of medical images of varied modalities, with the expectation that the composite enhanced output image generated by the system will aid the physician in a more prompt and accurate diagnosis of the medical condition being evaluated.

1.3 Review of Prior work

Wavelet transforms have quickly carved their niche in many research and applied fields, including telecommunications, biology, engineering, and medicine. These transforms have emerged as a powerful analytical tool whose prototype function is expanded, contracted, and shifted so as to optimally represent the signal under evaluation. In medicine, wavelets are nowadays utilized particularly for noise reduction, enhancement, and compression of one and two-dimensional signals. These applications [8-23] are discussed below.

Noise reduction and enhancement of images follows a multiscale edge representation first developed by Mallat and Zhong [8-9] and later expanded by Lu et al. [10]. The main idea of this approach is to construct an edge detector by defining two oriented wavelets as the multiscale gradient representation of a function in the horizontal and vertical directions. The multiscale edge points are characterized as the local maxima of the gradient magnitude at the specified scales. Noise reduction is based on eliminating edge points (high frequency components) that fall above thresholds defined by the user at the various scales [11]. This technique is applied in [12] to control blood vessel artifacts in brain function images, where the wavelet transform is used to analyze and later reconstruct the images without using the extrema from the regions of high variations/vibrations.

As in noise reduction, the enhancement of images is achieved by manipulation of their multiscale edges. The constrast of a medical image can be enhanced simply by stretching or scaling its multiscale gradient maxima [13], since they represent the intensity difference between different regions and features in the image at the given scales. This procedure has been applied successfully in the enhancement of MRI and CT images [11,13]. The greatest impact of this contrast enhancement technique has been in the early diagnosis of breast cancer [3,11,13-16]. Small tumors and microcalcifications are difficult to detect because of the similarity of normal glandular tissues to those afflicted by malignant disease [3]. Therefore, low-contrast mammographic images need to be rid of their inherent noise as well as enhanced at different levels of resolution to better characterize small lesions and other details. Nonlinear stretching of the wavelet coefficients of mammograms at various resolutions allows for simultaneous noise filtering and feature enhancement.

Finally, another main issue in medical imaging is data compression. Wavelets are specially suited for image compression since they are capable of concentrating the important information of an image in a relatively smaller number of coefficients [17]. The wavelet transform is successfully applied in the compression of noisy tomographic images in [3,18]. Other applications of wavelets in medical imaging [19-23] include image registration, local tomography reconstruction, MRI encoding and others.

Since the advent of fuzzy logic in the 1960's, many fuzzy techniques have been introduced for image analysis and processing. In the evaluation of medical data and images, fuzzy systems have been primarily designed for medical image segmentation, feature extraction and classification, noise filtering, image enhancement, and image fusion [24-27]. Reference [24] introduces a hybrid image modelling technique that utilizes mathematical morphology and fuzzy reasoning for segmentation and classification of myocardial images with a few fuzzy parameters. In reference [25], a fuzzy segmented version of a blurred chromosome image is extracted by an algorithm developed to minimize image ambiguity in both the intensity and spatial domain. A family of fuzzy inference operators is defined in [26] for the filtering and feature extraction of images. These operators perform fuzzy noise smoothing of a liver ultrasound image without loss of its structural content. Reference [27] presents a method for obtaining a high resolution PET image by correlating the radionuclide uptake of the original low resolution PET with the attenuation value in the corresponding CT or MRI image by fuzzy set theory.

Fusion of unimodal and multimodality images remains the subject of constant research in areas such as remote sensing and medical imaging. The fusion approach has been broadly defined by researchers over the years either as a visualization (2-D or 3-D), matching (registration), or actual data merging (combination) task. In this project, image fusion is determined as the merging of information from two or more input images in a product output image. An abundance of sources mention many techniques for the simultaneous visualization of medical images and for their matching, among which [1,2,28-30] provide a very comprehensive summary of the accomplishments in the area. Many references also discuss methods which perform fusion efficiently by combining data from multiple images in remote sensing [31-35], but fewer of them [24,26] propose schemes for fusion (as defined above) of multi-sensor medical images. Reference [24] presents an interesting technique that utilizes mathematical morphology to extract fuzzy features from multimodal images that are then identified as correspondent and fused by fuzzy reasoning. A discrete wavelet transform is applied in [36] for the decomposition of PET and MRI scans of the same patient. The wavelet coefficients are then compared by utilizing a simple maximization technique, and the resulting coefficient structure is reconstructed by the inverse wavelet transform in order to obtain the output fused image.

References [34-36] constitute the basic motivation for this project. There have been a very limited number of applications of the wavelet theory to the specific problem of medical image fusion. It is our intent to further investigate the suitability of wavelet transforms to the analysis of these type of images, as well as to introduce a new formulation to the selection criteria for fusion via fuzzy logic inference. No sources which combine wavelets and fuzzy logic to the fusion of images have been found in the literature.

1.4 Organization of the Thesis

This section describes the organization of subsequent chapters in the thesis. Chapter 2 of this thesis provides an overview of the fundamental theory of the discrete wavelet transform and multiresolution analysis as pertaining to the evaluation of two-dimensional signals. It also contains a discussion on the basic concepts and steps in the design of a fuzzy inference system. Chapter 3 presents a detailed description of the implementation of the proposed hybrid system for image fusion. It also describes the MATLAB™ wavelet and fuzzy toolboxes utilized in the design of the fuzzy-wavelet system and explains how they are integrated to perform the fusion of the images. Chapter 4 presents the results obtained with the proposed implementation, including a description of all images used to test the feasibility of the fusion system. Chapter 5 provides an overview of preprocessing techniques applied for image improvement when deemed necessary. This preprocessing stage is considered an auxiliary or secondary system to the fusion process. Conclusions and recommendations for future research are given in Chapter 6.

CHAPTER 2

BASIC THEORY

2.1 Introduction

In order to discuss the foundation and characteristics of the methods implemented in this work for image analysis, it is important to introduce a clear and formal definition of the term image. An image is a two-dimensional light intensity function $f(x,y)$, where x and y denote spatial coordinates and the value of f at any point (x,y) is proportional to the brightness (or gray level) of the image at that point [7]. For the purpose of analysis, a digital representation of an image is necessary. A digital image is an image $f(x,y)$ that has been discretized in spatial coordinates and in brightness, being represented by a matrix whose row and column indices identify a point in the image, while the corresponding matrix element depicts the gray level at that point. The elements that constitute this digital array are known as pixels. An interpretation of the information represented in the 2-D array is therefore the goal sought in the evaluation of images.

The analysis of images involves the identification or recognition of features in the 2-D signal such as smooth and sharp gray level transitions (edges), spikes, and other discontinuities, which are characterized either in the spatial and/or frequency domains. A transformation between these domains is therefore a routine task, performed to investigate whether the characteristics to be identified may be separated or isolated in either of these domains. This transformation is defined as a projection of the 2-D signal from its original domain to another one of choice, achieved through the use of a variety of mathematical operators. Many operators execute the projection (P) as shown below, by decomposing the signal into a sequence of analyzing functions

$$P = \langle f, \phi \rangle = \int_{-\infty}^{\infty} f \bar{\phi} \, dt, \tag{2.1}$$

where f is the image and ϕ is the analyzing function chosen. The selection of the analyzing function involves a search for a *basis* (collection of vectors $\{\mathbf{b}_1, \mathbf{b}_2, ..., \mathbf{b}_N\}$ such that any vector $\mathbf{u}$ may be written as a linear combination of the $\mathbf{b}_n$'s, i.e., $\mathbf{u} = \sum_n c^n \mathbf{b}_n$, and there is only one set of coefficients $\{c^n\}$ for which the linear combination may be done) that best describes the features of interest in the image. The choice of the basis depends on the characteristics of this 2-D signal and on the criterion selected for the portrayal of these features.

There are conditions which should be taken into account when selecting the adequate basis or analyzing function. Such conditions include: the orthogonality of the basis, the possibility of reconstructing the original image from its representation in the transform space, the stability and efficiency of the forward and inverse transformations, the ability of the basis to represent the image features in a sparse manner [37]. The following sections of the chapter address two operators which use different bases as their analyzing functions. The famous Fourier transform is briefly cited and characterized as a classical operator for the processing of images, and the concepts and theory of the wavelet transform are developed in support of its utilization for the image fusion task proposed in this thesis.

2.2 Brief Remarks on the Fourier Transform

The most common and widely used transform in image processing is the Fourier transform. Fourier analysis allows for the transformation of the view of an image from a spatial-based view to a frequency-based one by the decomposition of the image into constituent harmonic sinusoids (sine and cosines) of different frequencies. The main applications of the transform in image processing are in the enhancement and restoration of images.

The theory of Fourier analysis is developed in detail in [7], and interested readers are directed to this source for a complete exposition of equations and properties. The analyzing or bases functions (combinations of sine and cosines) of the Fourier transform cannot carry manageable spatial information due to their infinite support in the spatial domain [42]. This results in the inability of the localization of certain features in the image, since only global features are described well. Signals with many nonstationary characteristics such as abrupt changes (sharp edges) are not adequately described by the Fourier transform, and other techniques should be employed for an accurate analysis.

One such technique that provides both excellent frequency and spatial characterization of a signal is the wavelet transform [40]. The wavelet bases functions have compact support (vanish outside of a finite interval), therefore being localized in space. Another characteristic of wavelets is that they have an infinite set of possible bases functions, unlike the Fourier transform, which utilizes only the sine and cosine functions. In wavelet processing, if signal discontinuities are to be detected and a detailed frequency analysis performed, it is necessary to utilize a combination of short high-frequency basis functions and long low-frequency ones, which is how the wavelet transform is structured. Thus, access to features otherwise obscured by the Fourier transform is granted by wavelet analysis. Wavelets are formally introduced with a complete description of the fundamental equations in the sections that follow.

2.3 Wavelet Transform and Multiresolution Analysis

Wavelets, as defined by Daubechies [38], are mathematical functions that "cut up" data into different frequency components, and then study each component with a resolution matched to its scale. These functions satisfy the requirement that they should integrate to zero, "waving" above and below the x-axis [39]. Also, the diminutive connotation of the word also suggests it needs to be well localized.

Wavelets have a very interdisciplinary origin, having been independently developed in the fields of mathematics, physics, electrical engineering, and seismic geology. A. Haar mentions wavelets for the first time in the appendix to his thesis [38] in 1909. Between 1909 and 1980, many groups researched the representation of functions using scale-varying bases functions, an important concept to the development of wavelet theory. In 1980, Grossman and Morlet define wavelets in the context of quantum physics. Stephane Mallat discovers in 1985 some relationships between quadrature mirror filters (signal processing) and wavelet bases, which inspires Y. Meyer to construct the first non-trivial wavelets [40]. A few years later, I. Daubechies uses Mallat's work to construct a set of orthonormal basis functions, which are widely used in wavelet applications today. This section introduces the continuous and the discrete wavelet transforms, followed by the wavelet multiresolution approach to signal analysis.

2.3.1 Continuous Wavelet Transform (CWT)

The functions to be represented by a wavelet transform are those that are square integrable on the real line. They constitute a class that is denoted as $L^2(R)$. Therefore, the notation $f(x) \in L^2(R)$ signifies

$$\int_{-\infty}^{\infty} |f(x)|^2 dx < \infty \tag{2.2}$$

In wavelet analysis, a set of basis functions is obtained by dilating and translating a single prototype function or basic wavelet $\psi(x)$. This basic wavelet is an oscillatory function, usually centered upon the origin, which dies out rapidly as $|x| \to \infty$. Examples of wavelet prototype functions are shown in Figure 2.1. An extensive discussion on the continuous wavelet transform is provided in [38,41].

The prototype function $\psi(x) \in L^2$ has two characteristic components, namely the dilation or scale parameter a and the translation parameter b. This function $\psi(x)$ is translated and dilated in order to generate the set of wavelet basis functions $\psi_{a,b}(x)$ defined as

$$\psi_{a,b}(x) = \frac{1}{\sqrt{|a|}}\psi(\frac{x-b}{a}), \text{ with } a,b \in R \text{ and a} \neq 0 \tag{2.3}$$

The coverage of the time-scale plane by a wavelet prototype function is illustrated in Figure 2.2.

The continuous wavelet transform of a function in $L^2(R)$ is formally defined by

$$W_{a,b}(f) = \langle f, \psi_{a,b} \rangle = \int_{-\infty}^{\infty} f(x)\psi_{a,b}(x)dx \tag{2.4}$$

The reconstruction of $f(x)$ from its wavelet transform is made possible only if the Fourier transform of $\psi(x)$, $\hat{\psi}(\omega)$, satisfies the admissibility condition

$$C_\psi = \int_{-\infty}^{\infty} \frac{\left|\hat{\psi}(\omega)\right|^2}{\omega} d\omega \langle \infty \tag{2.5}$$

This condition implies that $\hat{\psi}(0) = 0$ and that $\hat{\psi}(\omega)$ is small enough near $\omega = 0$.

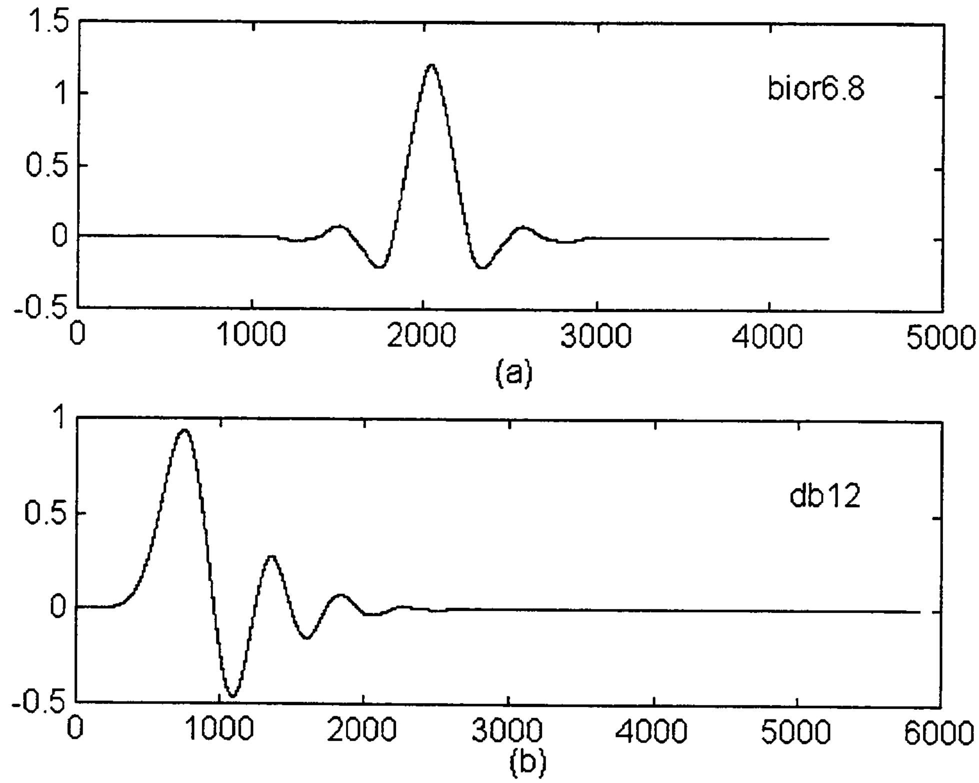

Figure 2.1. Examples of wavelet prototype functions. (a) biorthogonal wavelet, (b) Daubechies wavelet.

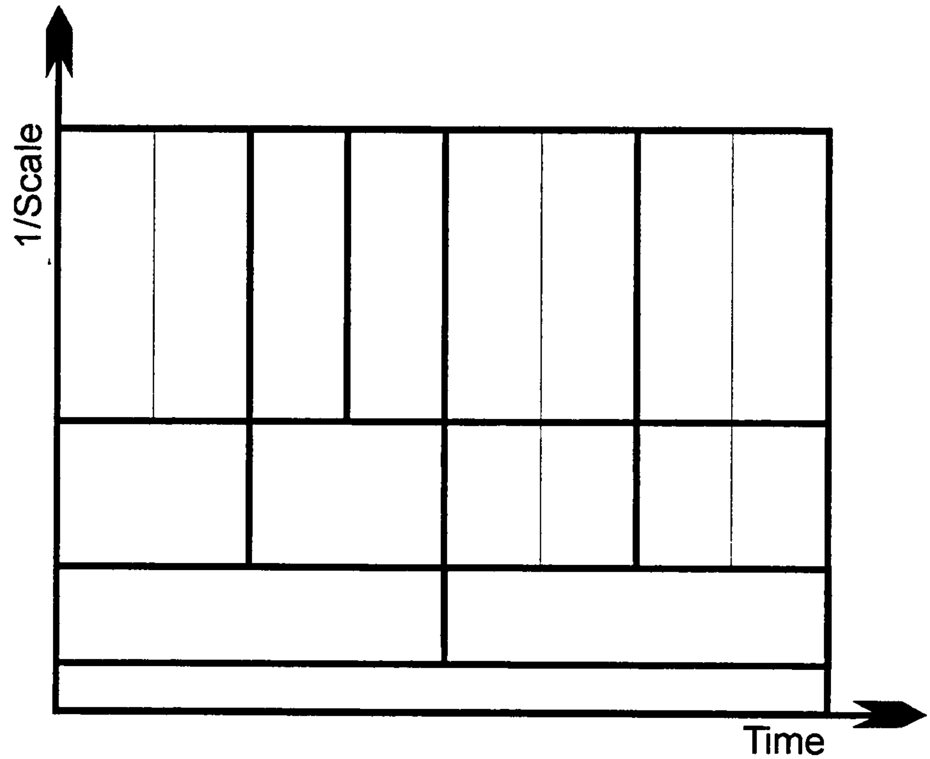

Figure 2.2. Coverage of the time-scale plane by a wavelet prototype function.

The continuous wavelet transform $W_{a,b}$ may then be inverted on its range, with the inverse transformation represented as

$$f(x) = \frac{1}{C_\psi} \iint_{-\infty} W_{a,b} \psi_{a,b}(x) \frac{da\,db}{a^2} \tag{2.6}$$

For functions of more than one variable, the dimensionality of the transform also increases. If $f(x,y)$ is a two-dimensional function, its continuous wavelet transform is

$$W_f(a,bx,by) = \int_{-\infty}^{\infty}\int_{-\infty}^{\infty} f(x,y)\psi_{a,bx,by}(x,y)dxdy, \tag{2.7}$$

where b_x and b_y specify the translation in two dimensions. The inverse 2-D CWT is described as

$$f(x,y) = \frac{1}{C_\psi} \int_0^{\infty}\int_{-\infty}^{\infty}\int_{-\infty}^{\infty} W_f(a,b_x,b_y)\psi_{a,b_x,b_y}(x,y)db_x db_y \frac{da}{a^3}, \tag{2.8}$$

where

$$\psi_{a,b_x,b_y}(x,y) = \frac{1}{|a|}\psi(\frac{x-b_x}{a},\frac{y-b_y}{a}) \tag{2.9}$$

and $\psi(x,y)$ is a 2-D wavelet prototype function.

2.3.2 The Discrete Wavelet Transform (DWT)

The representation of the continuous wavelet transform (CWT) is redundant, as implicit in its definition in Equation (2.4). For a given signal, it is possible to obtain a complete characterization of the CWT by its sampling in a dyadic grid. In this case, both the dilation parameter a and the translation parameter b take only discrete values

$$a = a_0^m$$
$$b = nb_0 a_0^m \tag{2.10}$$

where $m,n \in Z$, $a_0 \rangle 1$, and $b_0 \rangle 0$.

By substituting the above defined parameters in Equation (2.3), we obtain the wavelet prototype function

$$\psi_{m,n}(x) = a_0^{-m/2} \psi(a_0^{-m} x - nb_0). \tag{2.11}$$

The substitution of Equation (2.11) in Equation (2.4) yields the discrete wavelet transform

$$DWT(f) = \langle f, \psi_{m,n} \rangle = \int_{-\infty}^{\infty} f(x) a_0^{-m/2} \psi(a_0^{-m} x - nb_0) dx \tag{2.12}$$

The function $f(x)$ is then reconstructed with the inverse DWT as

$$f(x) = \sum_{m=-\infty}^{\infty} \sum_{n=-\infty}^{\infty} \langle f, \psi_{m,n} \rangle \hat{\psi}_{m,n} \tag{2.13}$$

We may also define $\psi_{m,n}$ such that it characterizes a function with good time-frequency localization properties by selecting special values for a_0 and b_0. Specifically, if we choose

$a_0 = 2$ and $b_0 = 1$, $\psi_{m,n}$ constitutes an orthonormal basis for $L^2(R)$ and is given by

$$\psi_{m,n}(x) = 2^{-m/2} \psi(2^{-m} x - n). \tag{2.14}$$

Wavelet prototype functions with these parameters were created by Daubechies [38], Meyer [42], and other researchers, each with different properties [42]. Stephane Mallat also based his formulation of an efficient DWT algorithm known as Multiresolution

Analysis on the study of an orthonormal wavelet basis with the same parameters listed above. The multiresolution wavelet representation originally developed by Mallat [42] constitutes one of the most famous and widely utilized wavelet techniques, and is presented in detail in the following subsection.

2.3.3 Multiresolution Analysis (MRA)

Multiresolution analysis is a technique utilized in the construction of orthonormal wavelet prototype functions of compact support for the analysis of 1-D or 2-D signals at different resolutions. A multiresolution analysis of $L^2(R)$ as defined by Chui in [44] consists of a sequence of closed approximation subspaces $\{V_m | m \in Z\}$ of $L^2(R)$, which has the following properties:

1. Containment: $V_m \subset V_{m+1}$,
2. Scaling: $f(x) \in V_m \Leftrightarrow f(2x) \in V_{m+1}$,
3. Shift invariance: $f(x) \in V_0 \Leftrightarrow f(x+1) \in V_0$,
4. Completeness: $\bigcup_{m=-\infty}^{+\infty} V_m$ is dense in $L^2(R)$ and $\bigcap_{m=-\infty}^{+\infty} V_m = \{0\}$,
5. There exists a scaling function $\phi(x) \in V_0$ such that

$$\phi_{m,n}(x) = 2^{\frac{-m}{2}} \phi(2^{-m}x - n) \tag{2.15}$$

characterizes an orthonormal basis for V_m, i.e.:

$$\int \phi_{m,n}(x)\phi_{m,n'}(x)dx = \delta_{n-n'} \tag{2.16}$$

where δ is the Kronecker symbol defined by:

$$\delta_{jk} = \begin{cases} 1, & j = k \\ 0, & \text{otherwise} \end{cases} \tag{2.17}$$

Since $\phi \in V_0 \subset V_1$ from the properties above, constants $h_n \in L^2(\mathrm{Z})$ exist such that the scaling function satisfies

$$\phi(x) = 2\sum_n h_n \phi(2\mathrm{x} - \mathrm{n}). \tag{2.18}$$

Equation (2.18) is known as either the dilation, refinement, or two-scale difference equation.

Furthermore, let us define W_m as the orthogonal complement of V_m in V_{m-1}, i.e.:

$$V_{m-1} = W_m \oplus V_m, \qquad V_m \perp W_m \tag{2.19}$$

The space W_m contains the "detail" information needed to go from an approximation at resolution m to an approximation at resolution $m+1$. Consequently,

$$\bigoplus_m W_m = L^2(R). \tag{2.20}$$

Since the wavelet prototype function ψ is an element of V_1, a sequence $g_n \in L^2(\mathrm{Z})$ exists such that

$$\psi(x) = 2\sum_n g_n \phi(2x - n). \tag{2.21}$$

Mallat discovered and showed in [43] that $h(n)$ in Equation (2.18) and $g(n)$ in Equation (2.21) are related to a lowpass filter $H(\omega)$ and a highpass filter $G(\omega)$ respectively, known as quadrature mirror filters in digital signal processing theory.

Based upon the previous discussions in this subsection, a signal $f(x)$ in V_m and W_m for finite m may be completely represented by

$$\begin{aligned} f(x) &= \sum_n c_{m,n}\phi_{m,n}(x) && \text{in } V_m \\ f(x) &= \sum_m \sum_n d_{m,n}\psi_{m,n}(x) && \text{in } W_m \end{aligned} \tag{2.22}$$

where

$$\begin{aligned} c_{m,n} &= \int f(x)\phi^*_{m,n}(x)dx \\ d_{m,n} &= \int f(x)\psi^*_{m,n}(x)dx \end{aligned} \tag{2.23}$$

Because $V_m = V_{m-1} \oplus W_{m-1}$, equation (2.22) can be rewritten as

$$f(x) = \sum_n c_{m_0,n}\phi_{m_0,n}(x) + \sum_{m=m_0}^{k-1} \sum_n d_{m,n}\psi_{m,n}(x), \quad k \rangle m_0 \tag{2.24}$$

Coefficients $c_{m,n}$ and $d_{m,n}$ are inner products between $f(x)$ and $\phi_{m,n}(x)$, and between $f(x)$ and $\psi_{m,n}(x)$, respectively. Therefore, the constants $c_{m,n}$ are approximation coefficients, while the constants $d_{m,n}$ are wavelet series coefficients. These $d_{m,n}$ and $c_{m,n}$ coefficients may be determined using the multiresolution analysis (MRA) algorithm developed by Mallat, which is available in the MATLAB wavelet toolbox. The 2-D version of the algorithm, which is utilized in this thesis for part of the analysis and processing of the images, is described in detail in [42,45]. A schematic overview of the steps that constitute the forward and inverse 2-D wavelet transformations as performed by Mallat's MRA scheme is provided in the next two subsections.

2.3.3.1 The 2-D Forward Wavelet Transform in the MRA Algorithm

We may characterize the input to the transform as an $N \times N$ image $f(x,y)$, where N is a power of two, $N = 2^m$, with m being an integer. For $m = 0$, the scale is $2^m = 2^0 = 1$, which is the scale of the original image. Each larger integer value of m doubles the scale and halves the resolution. Since the variables in the 2-D representation may be treated independently, the 2-D scaling and wavelet functions are considered separable.

In the 2-D algorithm, the wavelet prototypes and scaling functions are obtained from 1-D wavelets by tensorial product. At each stage of the transform, the image is decomposed into four quarter-size images, as shown in Figure 2.3. Each of the four quarter-size images is formed by first convolving the rows of the image $f(x,y)$ with the lowpass filter function $h_0(-x)$ and with the highpass filter function $h_1(-x)$ (both derived according to the wavelet prototype chosen), and subsequently discarding the odd-numbered columns of the two resulting arrays [45]. The columns of each of the $N/2 \times N$ arrays are then convolved with $h_0(-x)$ and with $h_1(-x)$, and the odd-numbered rows are discarded. The result is the four $N/2 \times N/2$ arrays required for that stage of the transformation, and the described process is diagrammed in Figure 2.4.

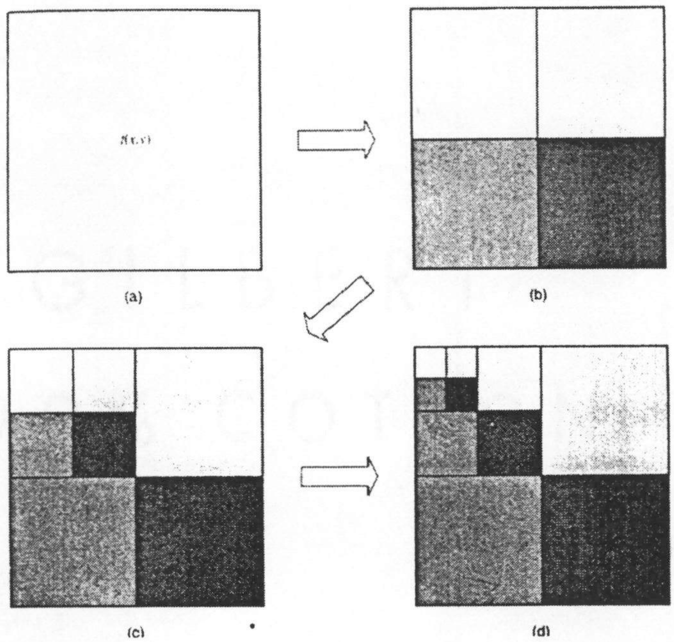

Figure 2.3. The 2-D discrete wavelet transform decomposition steps [45].

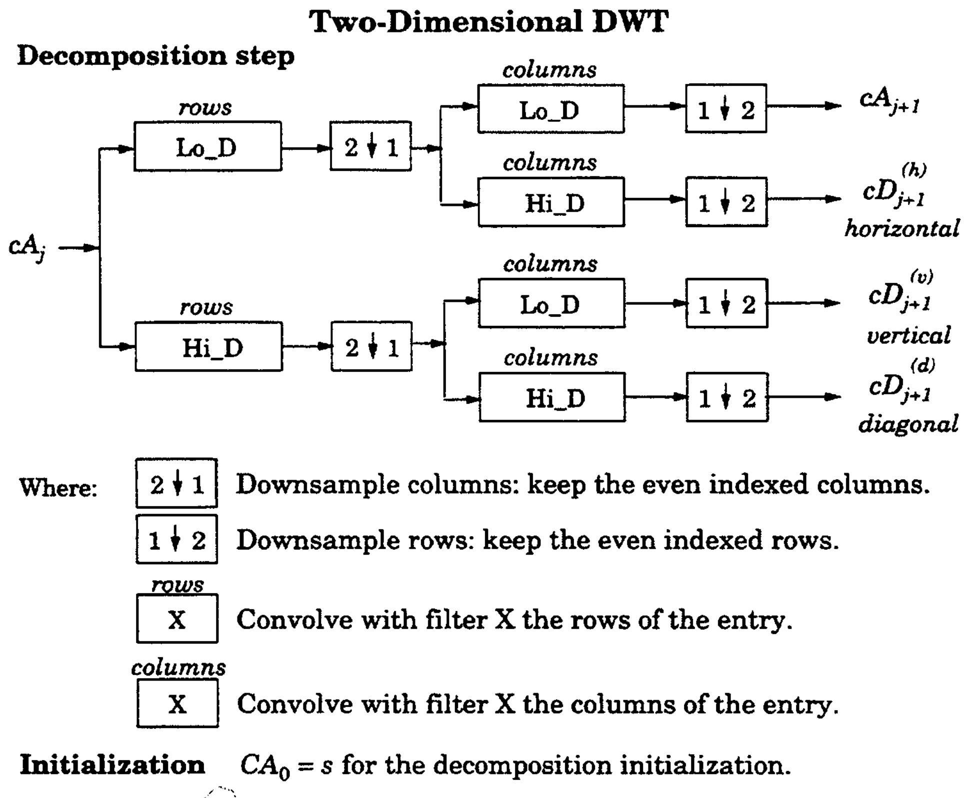

Figure 2.4. Wavelet toolbox 2-D forward discrete wavelet transform [42].

The transform procedure may be carried to J stages, where the integer $J \leq \log_2(N)$ for an $N \times N$ pixel image. Thus, the two-dimensional separable DWT may be computed quickly. If the transformation coefficients are calculated with floating-point accuracy, the inverse transform can reconstruct the original image with little degradation. The 2-D MRA inverse wavelet transform process is briefly explained next.

2.3.3.2 The 2-D Inverse Wavelet Transform in the MRA Algorithm

Inversion of the discrete 2-D wavelet transform in MRA is done by a process similar to the forward transformation outlined above. The procedure is schematized in Figure 2.5. At each stage (e.g., the last), the four previous stage arrays are upsampled by inserting a column of zeros to the left of each column [45]. The rows are then convolved with either the lowpass $h_0(x)$ or the highpass $h_l(x)$ filter functions, and the $N/2 \times N$ arrays are added in pairs, as depicted in Figure 2.5. Subsequently, the columns of these two arrays are convolved with $h_0(x)$ and with $h_1(x)$, and the sum of the two resulting arrays is the result for that stage of the reconstruction process. The algorithm is repeated until a final reconstructed image is obtained. An adequate reconstruction of the original image is the goal of the 2-D inverse wavelet transform procedure.

2.3.3.3 Discrete Wavelet Packet Transform Analysis

The wavelet packet framework is a generalization of the wavelet transform decomposition, more versatile in its signal and image analysis procedure.

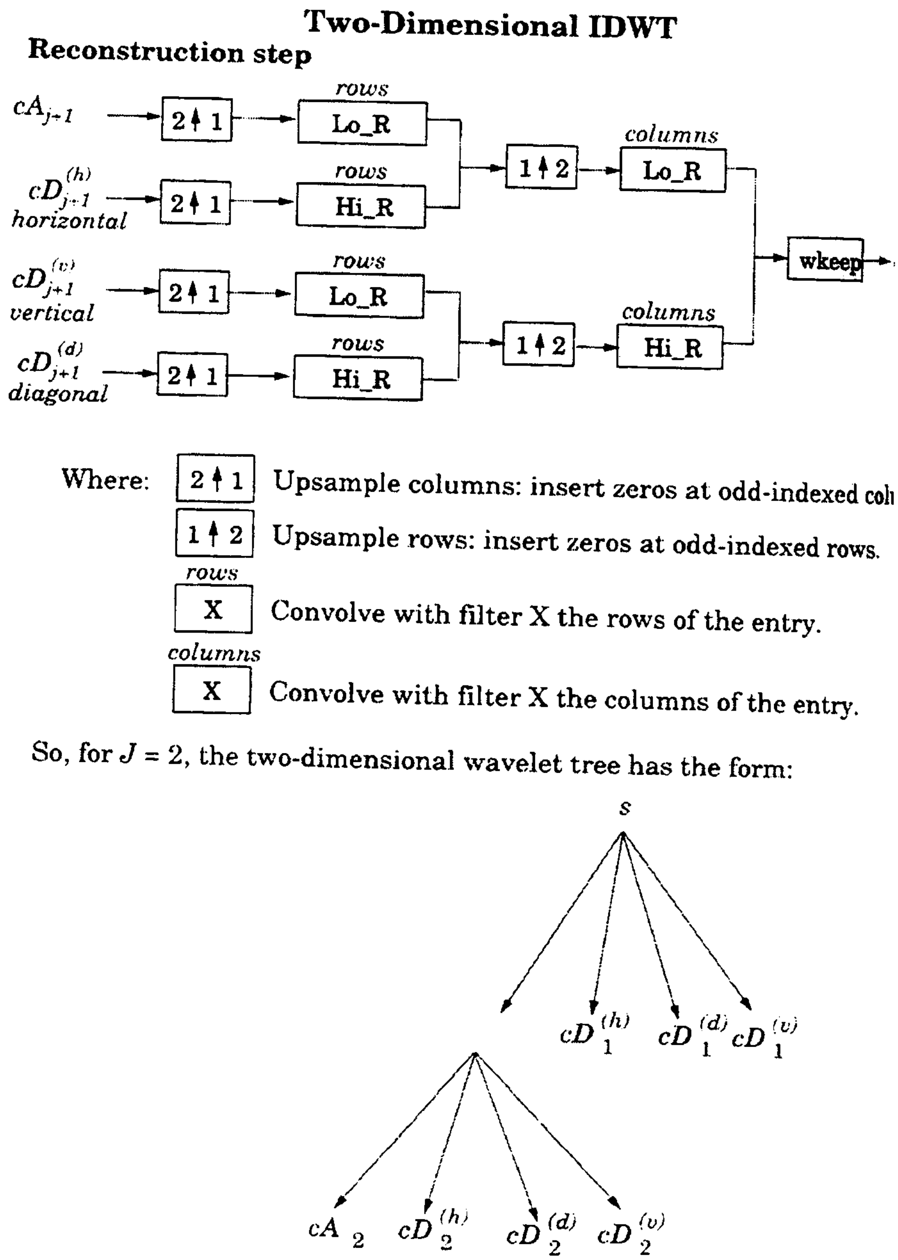

Figure 2.5. Wavelet toolbox 2-D inverse discrete wavelet transform [42].

While the standard orthogonal wavelet decomposition procedure splits only the wavelet approximation levels successively, the wavelet packet also splits the corresponding detail coefficient vector into its constituent parts, utilizing the same approach as in the approximation vector splitting.

The wavelet packet basis functions, also known as wavelet packet atoms, are particular linear combinations of wavelet prototype functions with the implicit orthogonality and localization properties of their parent wavelet. Each basis offers a specific way of coding a signal, preserving its global energy and providing a great reconstruction of its features. A large number of wavelet basis expansions are generated upon a single wavelet packet signal decomposition, and then the best representation of the decomposed 1-D or 2-D signal may be selected based on the entropy minimization criterion.

The MATLAB wavelet toolbox contains an algorithm for both wavelet packet decomposition and optimal signal decomposition representation. The decomposition results offer a richer and more complex analysis than the one obtained with the wavelet framework, which may provide more insight into details characterized in the detail coefficient vector, if it suits the design objective. In the particular case of this thesis, the wavelet packet framework capabilities are not utilized in their full potential, since the design objective is met by the analysis of the approximation coefficient vector only, due to the specific nature of the images being evaluated and of the hybrid technique implemented.

2.4 The Fuzzy Inference System (FIS)

Fuzzy logic applications have rapidly grown in their number and variety since the development of the basic fuzzy logic theory by Zadeh [46] in the late 1960's. The overwhelming acceptance of fuzzy logic in real systems applications is due to its ability to address intrinsic vagueness in physical systems thorough a flexible reasoning which imitates the human decision making ability. A constituent technique of what may be referred to as "soft computing" [47], fuzzy logic incorporates a tolerance for imprecision and partial truths in order to provide tractable, robust, and low-cost solutions in scientific and industrial areas such as control systems, robotic vision, and signal processing, among many others. In this respect, the aim in this thesis is to illustrate and verify the application of the fuzzy technique in the evaluation of 2-D signals, and specially, in the fusion of medical images. Since fuzzy logic involves a broad range of concepts, only the theory related to the design of the proposed hybrid system is exposed and discussed in this section.

2.4.1 Basic Concepts

Fuzzy logic inferencing may be defined as a convenient method for mapping an input space to an output space. Some advantages of this technique include the ease of understanding its concepts due its simplicity as a method based on natural language, its flexibility in the representation of data, its tolerance of imprecise measurements, its ability to model nonlinear functions of arbitrary complexity, and its capability of blending with different conventional techniques for their augmentation or simplification [47].

The main idea is to interpret the values in an input vector and, based on a set of rules composed of if-then statements, assign values to a corresponding output vector. All rules are evaluated in parallel, and their functionality is characteristic of the manner in which they refer to the variables in the system and the adjectives that describe those variables. The order of the rules is not important in the analysis of the data. Before designing a strategy to interpret these rules, it is necessary to define the input(s) and output(s) of the system, that is, the variables, and the terms that describe them.

The input variables are the precise or crisp measurements that are to be evaluated or mapped by the fuzzy system, while the output variables are the resultant precise values originated by the fuzzy processing of the corresponding input measurements. The steps involved in this fuzzy processing comprise the fuzzification of the input variables, the application of the fuzzy operator in the antecedent, the implication from the antecedent to the consequent, the aggregation of the consequents across the rules, and defuzzification [47]. All these steps are cited and explained in the next subsection of the present chapter.

For the system implemented in this work, there are two inputs, namely, the MRI wavelet coefficient and the corresponding PET wavelet coefficient. The output variable corresponds to the fused wavelet coefficient obtained with the combination of the input variables determined by the rules of the fuzzy engine. The input space, also referred to as the universe of discourse, is defined for both inputs as ranging from $-\Delta$ to Δ, where $\Delta = \max\{\max(abs(\text{MRI wavelet coefficients})), \max(abs(\text{PET wavelet coefficients}))\}$. The output space is also characterized by the range mentioned above.

Fuzzy sets are defined in both input and output domains. They may be described as sets without crisp, clearly defined boundaries, which may contain elements with only a partial degree of membership. Therefore, these sets describe vague concepts, such as the set of small wavelet coefficients in our implementation. They are defined by curves that determine how each point in the input space is mapped to a membership value. The curves are named membership functions, and they portray the degree to which a certain input belongs to a specific fuzzy set. The membership value or degree of membership must vary between 0 and 1, and the function itself can be an arbitrary curve whose shape may be characterized according to the system design objective, from the point of view of simplicity, convenience, and efficiency. An illustration of a fuzzy set and corresponding membership functions which define one of the input domains in our implementation is shown in Figure 2.6.

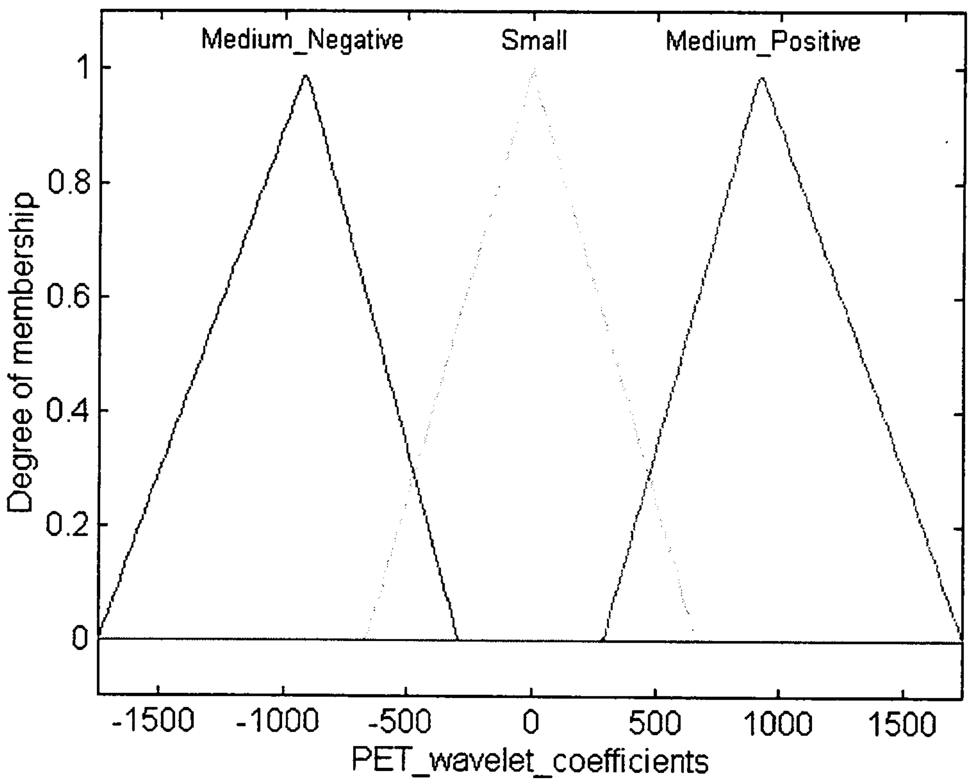

Figure 2.6. Illustration of a fuzzy set and membership functions for an input variable.

In order to evaluate data with the particular design of the parameters introduced above (fuzzy sets and their characteristics), rules need to be created and introduced in the fuzzy system for the accurate portrayal of the task we wish to accomplish with the design. These rules comprise if-then conditional statements that utilize fuzzy operators to establish the correspondence between the logical operations defined in the rules. There are three types of fuzzy operators that may be defined and utilized in building if-then rules: the fuzzy intersection or conjunction (AND), fuzzy union or disjunction (OR), and the fuzzy complement (NOT) [47]. Typically, AND and OR operators can easily be customized for the particular fuzzy system being implemented. The fuzzy sets and fuzzy operators may be considered the "subjects" and "verbs" of fuzzy logic [47].

If-then rules present the following general form:

if x is A *then* y is B,

where A and B are linguistic values defined by fuzzy sets on the ranges (universe of discourse) X and Y, respectively. The if-part of the rule "x is A" is called the antecedent or premise, while the then-part of the rule "y is B" is known as the consequent or conclusion. Conditional statements may have multiple antecedent and/or multiple consequents. The antecedent is an interpretation that returns a single number between 0 and 1, whereas the consequent is an assignment that assigns the entire fuzzy set B to the output variable y. So, the input to an if-then rule in the designed fuzzy system is the current value for the input variable (A), and the output is an entire fuzzy set (B).

After the fuzzy sets, membership functions, fuzzy operators, and if-then rules have all been defined for the design of a certain fuzzy system, a stage of evaluation of the fuzzy rules follows. The interpretation of if-then rules is a three part process, which comprehends the fuzzification of inputs (evaluating the antecedents), the application of fuzzy operators, and the utilization of an implication method (applying the result of the input evaluation to the consequent). Finally, the fuzzy sets resulting from the interpretation of the system rules need to be transformed into a single crisp result for the output variable.

The last stage is accomplished by the aggregation of the output fuzzy sets for each rule into a single set, and the subsequent deffuzification of this resulting output fuzzy set into a single number. The steps to be followed in the design of a fuzzy inference system are explained in the next subsection of this chapter.

2.4.2 Steps in the Fuzzy Inference Process

Fuzzy inference is the actual process of mapping from a given input to an output using fuzzy logic. The process involves all the concepts discussed in the previous section, namely fuzzy sets, membership functions, fuzzy logic operators, and if-then rules. There are two main inference procedures that may be utilized in fuzzy logic applications: generalized modus ponens (GMP) and generalized modus tollens (GMT) [46]. In this work, the GMP technique that uses a rule, a particular condition, and evaluates the corresponding particular conclusion, is the choice of inferencing selected. Furthermore, different inference styles are available for the design of a fuzzy system, such as the Mamdani and Sugeno methods. A Mamdani-style fuzzy inference method is chosen for the design of our system, since for this style the output membership functions are distributed fuzzy sets, not a single spike as in the case of a Sugeno fuzzy model. The interested reader is refered to [47] for further details.

As mentioned in the previous section, a fuzzy inference process may be characterized in five parts: fuzzification of the input variables, application of the fuzzy operator in the antecedent, implication from the antecedent to the consequent, aggregation of the consequents across the rules, and defuzzification. The fuzzy logic toolbox [47] employed in this thesis supports these same structural steps for the creation of a fuzzy inference system. The characteristic stages of the fuzzy system design are summarized below:

- Fuzzify Inputs - This first step consists of taking the inputs and determining the degree to which they belong to each of the appropriate fuzzy sets via membership functions. The input is always a precise numerical variable limited to the universe of discourse of the particular input variable, whereas the output is a fuzzy degree of membership between 0 and 1.
- Apply Fuzzy Operator - Upon fuzzification, the degree to which each part of the antecedent has been satisfied for each rule is known. When the antecedent of a given rule

has more than one part, a fuzzy operator (AND or OR) needs to be applied in order to obtain one single number that represents the result of the antecedent for that rule. The input to a fuzzy operator is two or more membership values from fuzzified input variables, and the output is a single truth value.

- Apply Implication Method - If a certain rule is assigned a specific weight (optional implementation parameter), this weight must first be applied to the truth value given by the corresponding antecedent. Then, the implication method selected shapes the consequent (a fuzzy set) based on the antecedent (single number). Implication occurs for each rule, and many methods are available for implementation, as described in [46]. The most popular ones are Mamdani's "min" (utilized in this work), which truncates the output set, and Larsen's "prod", which scales the output fuzzy set. The input for the implication process is a single number given by the antecedent, whereas the output is a fuzzy set.

- Aggregate All Outputs - Aggregation consists of taking all the fuzzy sets that represent the output of each rule and combining them into a single fuzzy set. It only occurs once for each output variable. The list of truncated output functions returned by the implication process for each rule constitutes the input of the aggregation stage, while the output is characterized by one fuzzy set for each output variable. Popular aggregation methods include the "max", "probor" (probabilistic or), and "sum", as described in [47]. In the scope of this thesis, we selected the "max" aggregation technique for the design of the inference system.

- Defuzzify - Defuzzification implies the final move from a fuzzy set to a crisp output. It involves the transformation of each output variable fuzzy set to a single and precise number, which is the final output of a fuzzy inference system. The most common defuzzification technique and the one selected in our implementation is the centroid calculation, which returns the center of area under a resulting curve [47].

CHAPTER 3

SYSTEM IMPLEMENTATION

3.1 Overview

The system implemented as part of this work was designed to provide an alternative technique for the fusion of medical images by combining fuzzy logic and wavelet technology. In the context of this thesis, fusion signifies the merging of data from two or more input images in a product output image, as specified in a discussion earlier in Chapter 2. An illustration of the general components utilized to build the proposed system is shown in Figure 3.1. The goal in the implementation phase was to develop the methodology with software that is supported in different computational environments and easily transferred across platforms. All fusion system components were implemented in MATLAB by utilizing the many toolboxes [42,47] developed specifically for signal and image processing within this software.

The preprocessor displayed in Figure 3.1, which comprises different algorithms that may be applied to the improvement of images prior to their fusion, is treated as an auxiliary or secondary system. This preprocessing system is addressed in Chapter 5. A diagram of the basic implementation steps for the fusion of medical images is given in Figure 3.2. The fusion system developed in this thesis is presented in detail in the subsequent sections of this chapter.

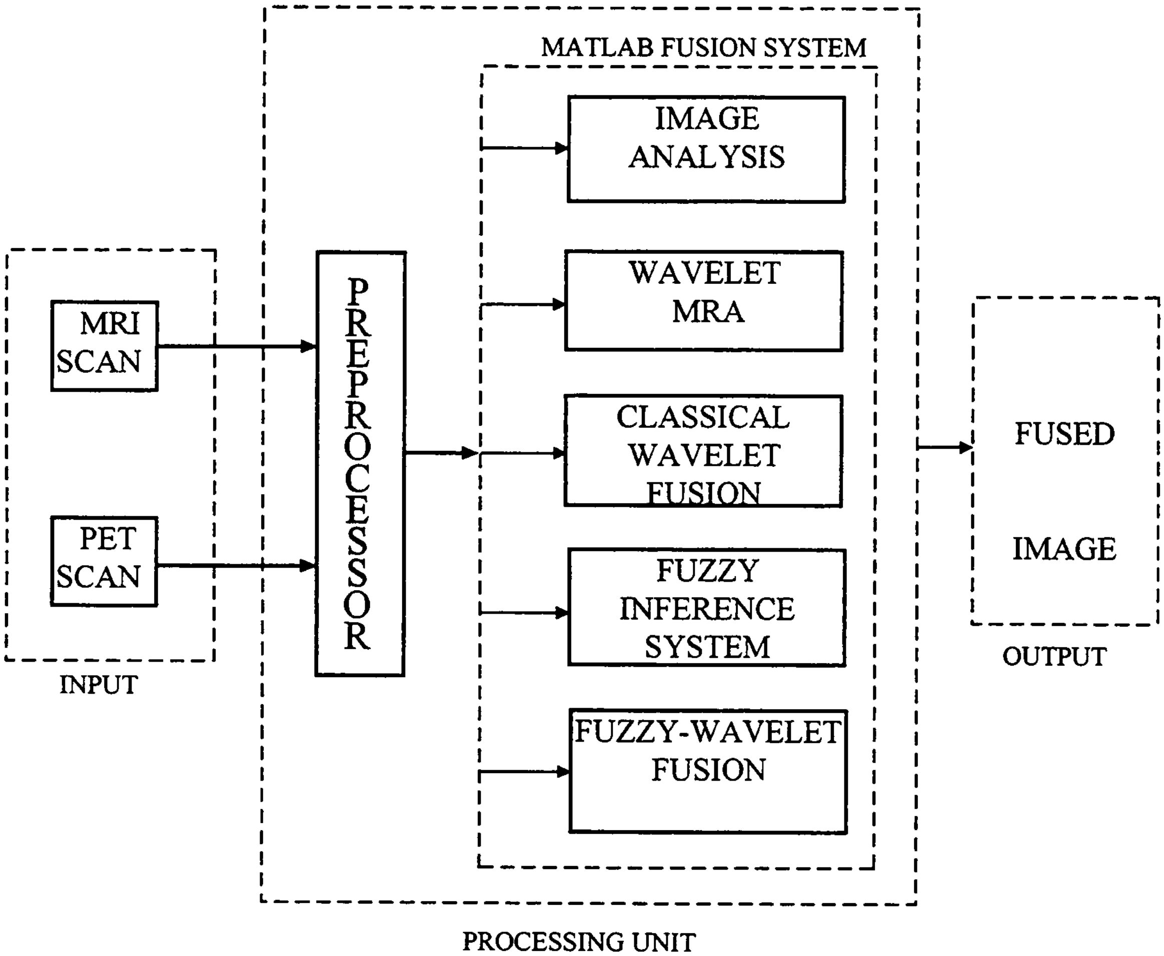

Figure 3.1. Diagram of system components.

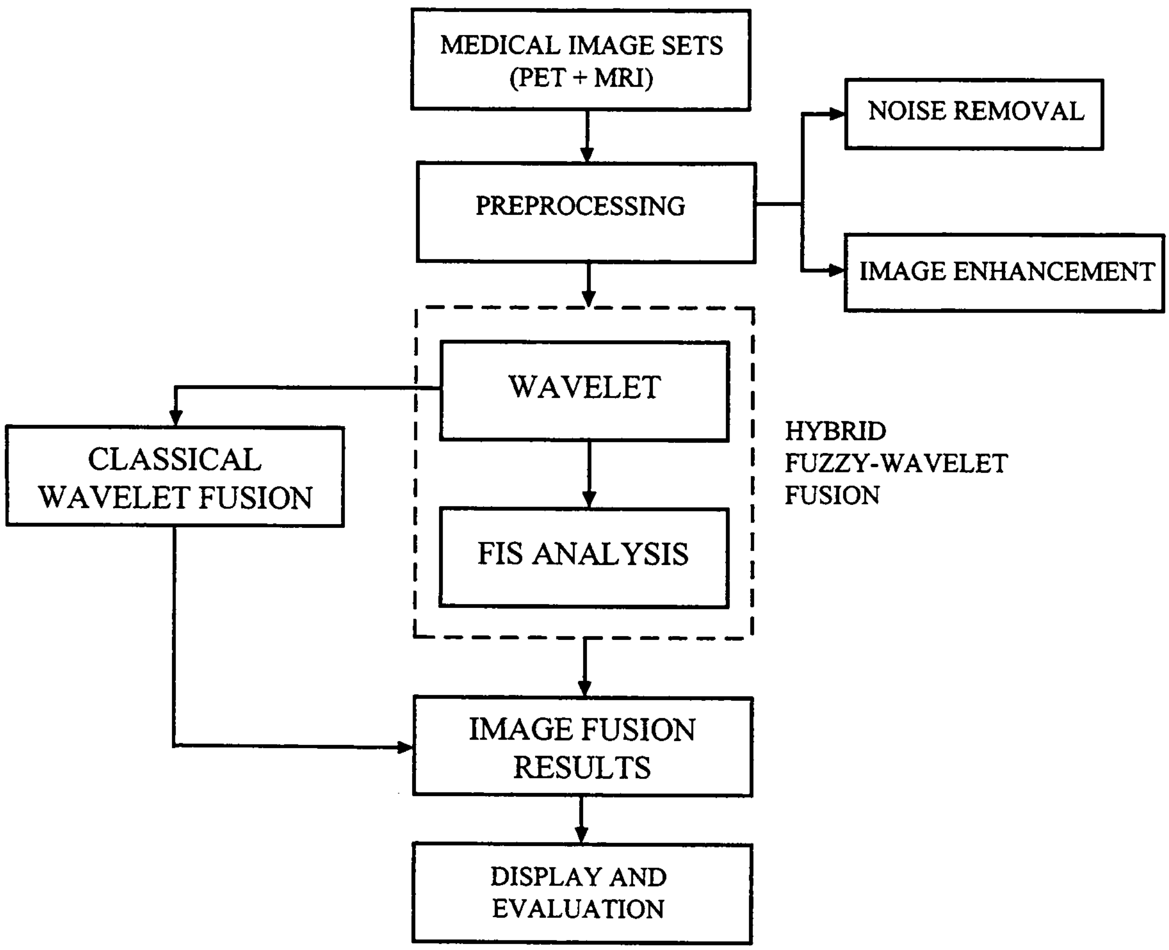

Figure 3.2. Diagram of the fusion system implementation steps.

A basic outline of the procedures, which indicate the algorithms implemented and the parameters chosen at each step of the fusion process, is provided as a guide to the analysis and understanding of the results provided in Chapter 4.

3.2 Image Fusion System

For fusion, the MATLAB wavelet toolbox is extensively utilized for the processing of the pertinent images within the wavelet packet framework. The classical wavelet fusion approach is implemented with the features of the 2-D wavelet packet analysis. The MATLAB fuzzy inference system (FIS) toolbox is used in conjunction with the wavelet toolbox for the development of the hybrid fuzzy-wavelet technique. The next subsections present the toolboxes used in this methodology, and show the implementation of the fusion through the classical and hybrid methods. Fusion of the preprocessed images is accomplished in two stages: during the first, wavelet transforms are calculated for the image data; in the second stage, wavelet coefficients are combined with fuzzy inferencing.

3.2.1 MATLAB Wavelet Toolbox Description

The wavelet toolbox is a collection of functions built on the MATLAB platform. The toolbox is designed for the analysis of 1-D and 2-D signals using wavelets and wavelet packets. There are two categories of tools provided for data evaluation, one is line driven, the other is based on a graphical user interface (GUI). An example of the functionality of the graphical interface tool in the analysis of a medical image is given in Figure 3.3. This figure shows the wavelet packet evaluation of a PET image of the brain. A biorthogonal 3.7 basis function is selected, and the decomposed image is shown in terms of all coefficient matrices that constitute the wavelet tree representation. Although this graphical interactive tool is excellent for the visualization of the analysis, the command line tools were chosen for system implementation. This choice provided an increased flexibility in the direct manipulation of selected wavelet coefficient matrices for the fusion of the specific images in our data sets. Batch programs of command line functions are written for the execution of various tasks. These programs are explained in detail as the methodology is presented.

The wavelet packet framework is selected for all analyses performed in this work. Through experimentation, it was observed that the fuzzy-wavelet fusion of the medical images evaluated in this thesis is best performed by utilizing only the matrix of wavelet approximation coefficients at the chosen level of decomposition. The images are very well characterized by the information content represented in these coefficients. Detail coefficient matrices are, therefore, not included in the reconstruction and fusion of the images with the fuzzy-wavelet scheme, since they do not contribute any additional information relevant to the fusion task.

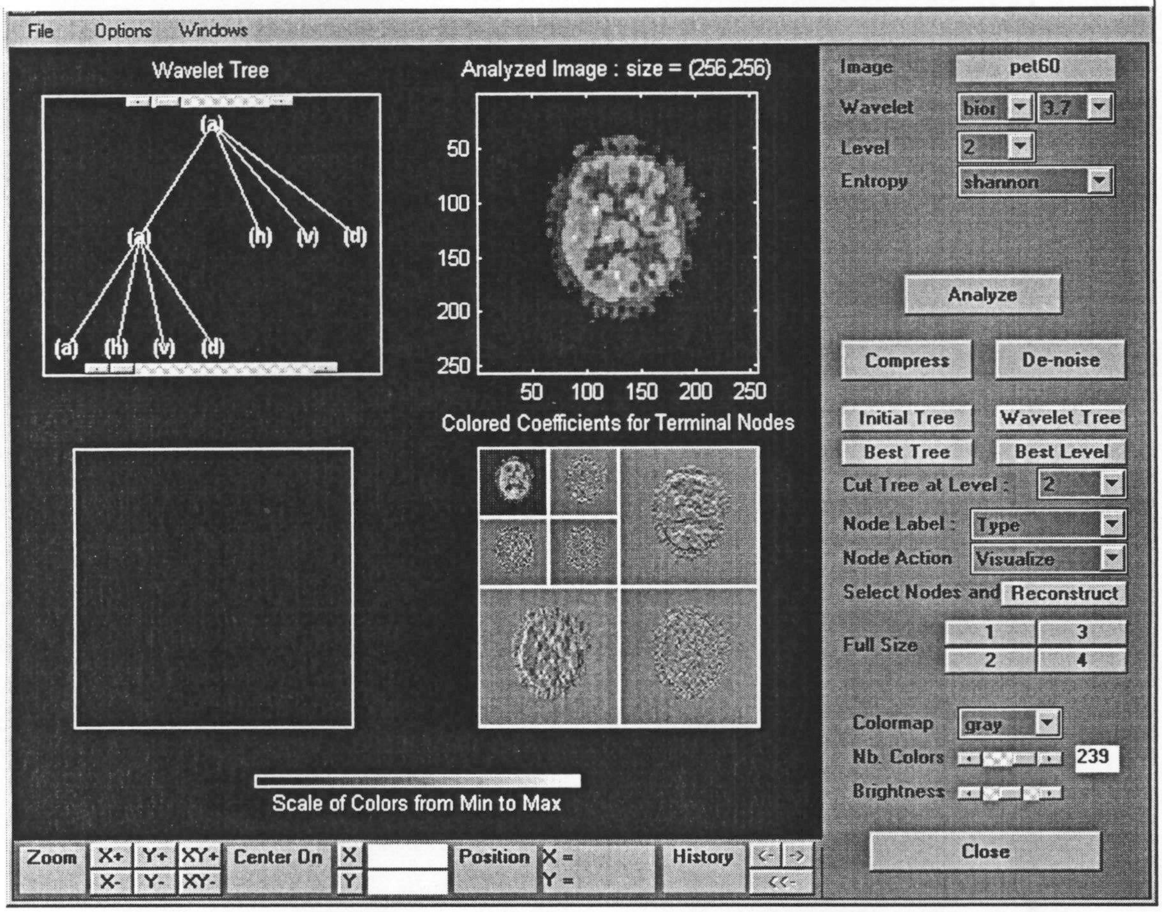

Figure 3.3. Wavelet packet evaluation of a PET image of the head [51].

A complete report of the functionality provided in the wavelet toolbox can be found in reference [42]. We present here a description of the functions that were used within the scope of this work.

Also included are algorithms developed under this project for the implementation of image fusion. The discussion that follows is based on two different techniques utilized for the fusion of multimodal images: the first is a classical method involving the integration of wavelet coefficients, the second consists of the proposed hybrid fuzzy-wavelet procedure.

3.2.2 Classical Wavelet Fusion Implementation

The classical wavelet fusion scheme as documented in [36] introduces the notion of fusing two or more images by applying a wavelet transform to them, combining their wavelet coefficients, and producing the output fused image by computing the inverse wavelet transform of the fused coefficients. The main issue in the implementation of the technique is the selection of the rule for integrating the wavelet coefficients from the different images. Reference [36] proposes the selection of the wavelet coefficients whose absolute values are higher at every point in the transform domain. This procedure is known as the "max" rule.

Different fusion rules are cited in [35], which introduce a variety of operators for the manipulation of the wavelet coefficients upon their combination. The wavelet fusion with the "max" rule was implemented as part of this research work as a means of validating and comparing our results. The code for this implementation is included in Appendix A, Program 1. The procedure is outlined below:

1. The coregistered PET and MRI images are loaded into MATLAB. A synthetic image filled with zeros, which will later store the data structure of the fused image, is created and loaded at this stage;
2. A biorthogonal 3.7 (bior 3.7) basis function is selected to perform a 2-D wavelet packet decomposition of the loaded images in 3 levels. The wavelet packet tree structure of one of these images is displayed in Figure 3.4;
3. A wavelet tree structure (Figure 3.5) is obtained by the recomposition of the nodes that represent the matrices of detail coefficients in the first and second decomposition levels. The structure that contains the data is automatically updated;
4. All matrices of detail and of approximation coefficients of each image are read and stored in separate matrices for further processing;
5. The "max" rule is implemented for the fusion of each set of wavelet coefficients. A normalization of the boundaries of these wavelet coefficients for the fusion with the "max" rule is an available option frequently used. The normalization factor promotes feature enhancement and is defined as:

   $\max(abs(MRI \text{ wavelet coefficients}))/\max(abs(PET \text{ wavelet coefficients}))$;

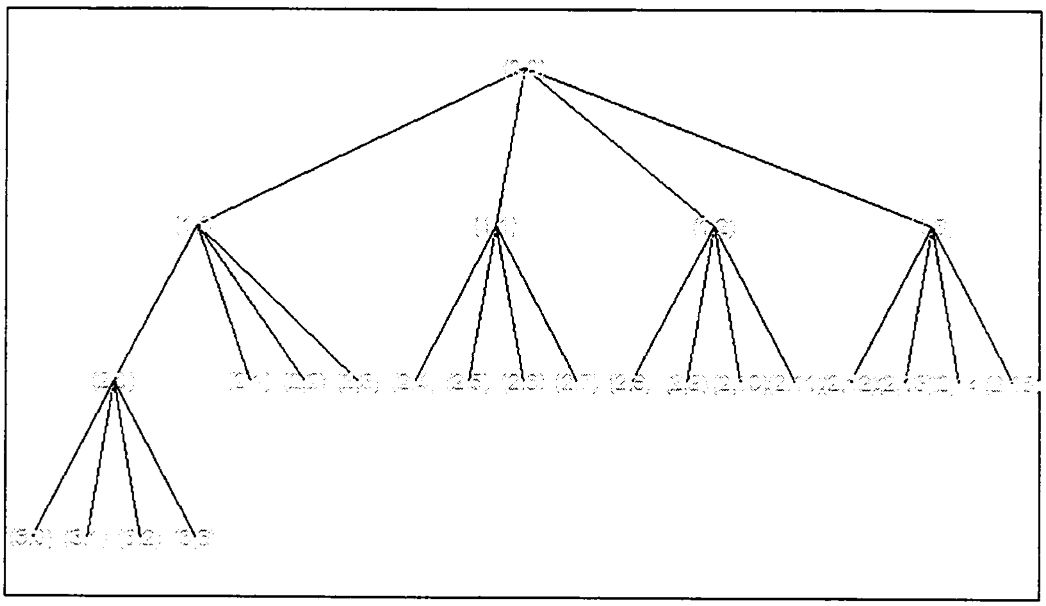

Figure 3.4. Partial display of a wavelet packet tree structure.

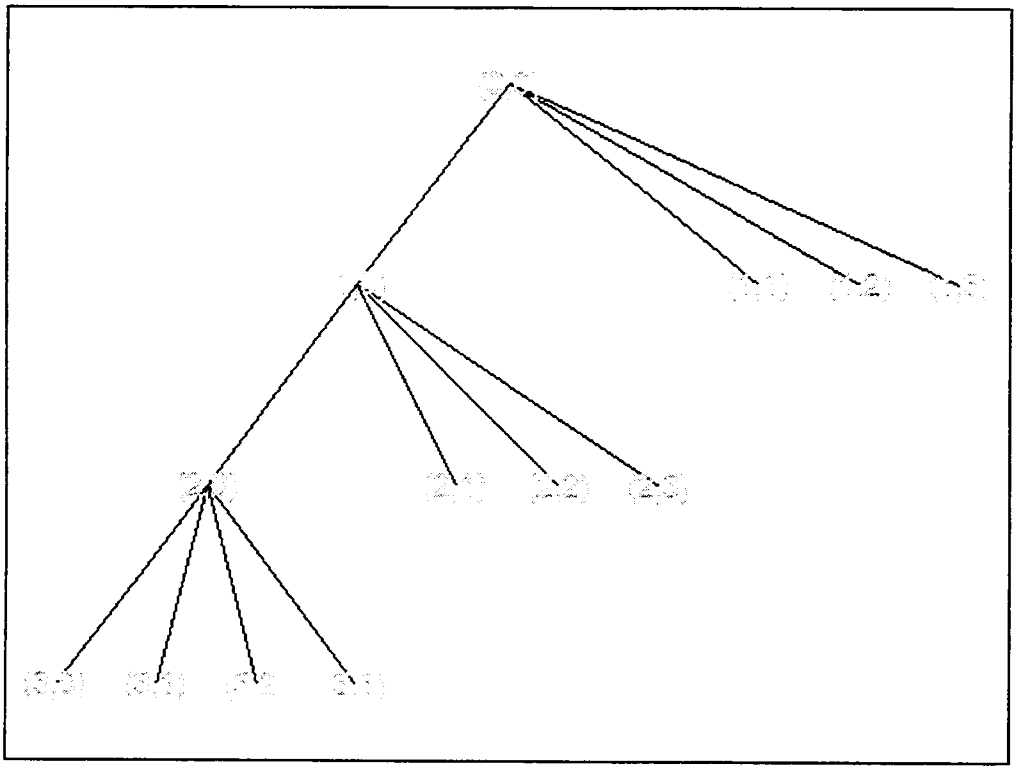

Figure 3.5. Wavelet tree obtained after recomposition of nodes.

6. The fused wavelet coefficient matrices are stored in the data structure of the synthetic image, which is then reconstructed with the inverse wavelet packet transform, in order to obtain the resultant fused output image;
7. The fused output image is displayed for visual evaluation.

3.2.3 MATLAB Fuzzy Logic Toolbox Description

The MATLAB fuzzy logic toolbox is, as its wavelet counterpart, a collection of tools built on the MATLAB environment for the design of fuzzy inference systems (FIS). Both command line and graphical interface tools are provided as options for data analysis. The building and editing of fuzzy systems is greatly facilitated by the five primary GUI's available for this purpose: FIS editor, rule editor, membership function editor, rule viewer, and surface viewer. The FIS editor handles the assignment of the general features of the fuzzy system, such as the input and output variables and the style of inference; the rule editor provides the environment for the determination of the rules that model the behavior of the system; the membership editor allows for the flexible definition of the shapes of the membership functions; and the rule and surface viewer are read-only tools for the observation of system components and their corresponding behavior.

The primary parameters that influence the outcome of the fuzzy system designed with the above GUI's comprise the style of inference selected for the modelling of the system; the adjustment of the fuzzy inference functions (i.e implication, aggregation, and defuzzification) applied; the shape and number of the fuzzy membership functions; and the number and style of inference rules, including the fuzzy operators that determine how these rules handle the data. In the present work, all these parameters are selected and combined in a hybrid scheme that fuses medical images.

A Mamdani-style fuzzy inference method [47] is utilized. This is done because the output membership functions need to be characterized as a distributed fuzzy set for the representation of the image data. The fuzzy inference functions are set in the FIS editor as "min" (Mamdani's min) for the implication method, "max" for the aggregation method, and "centroid" for the deffuzification method. Furthermore, five triangular membership functions (MF) are initially built to define the shape of the primary values (LN = large negative, MN = medium negative, SM = small, MP = medium positive, LP = large positive) for the two inputs and the output of the fuzzy system. This configuration is illustrated in Figure 3.6.

The input linguistic variables [46] represent the set of MRI and PET wavelet coefficients to be fused, while the output linguistic variable models the fused output image. All share the same universe of discourse, ranging from $-\Delta$ to Δ, where

$\Delta = \max\{\max(abs(\text{MRI wavelet coefficients})), \max(abs(\text{PET wavelet coefficients}))\}$.

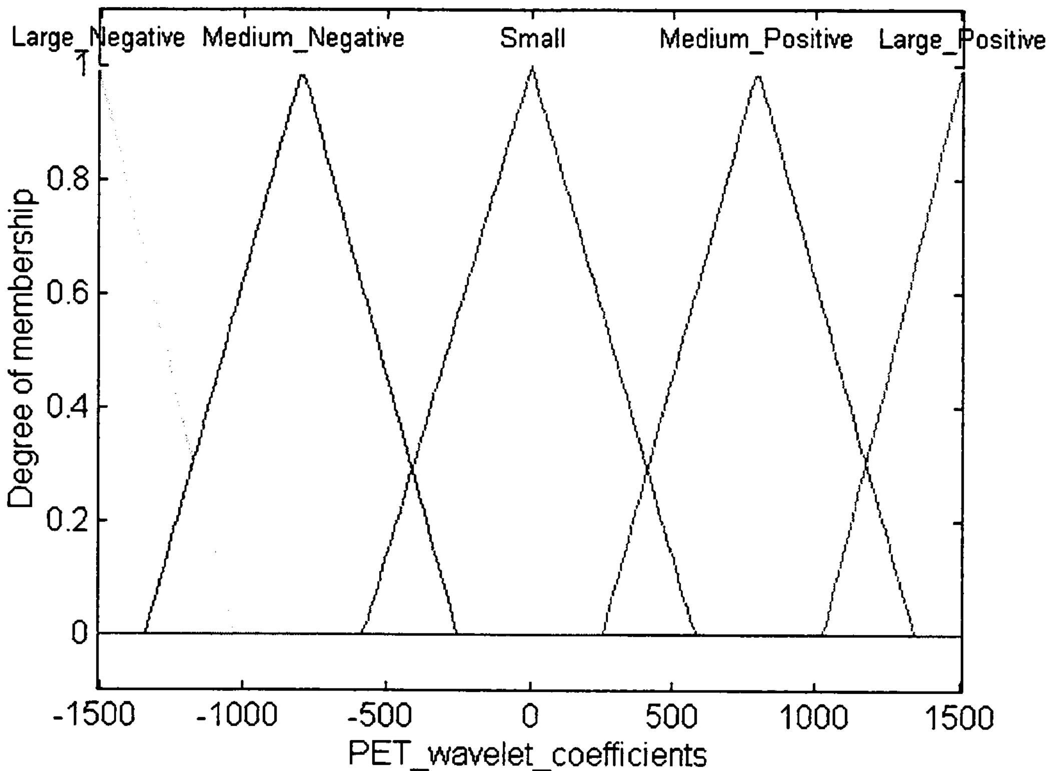

Figure 3.6. Initial membership function design associated with the input and output variables.

Upon experimentation with the fusion scheme, the number of triangular membership functions defining the primary values for the inputs and output of the system is reduced to three, as shown in Figure 3.7. The inherent nature of the data being modeled allows for as accurate a characterization of the relevant image features with three (MN = medium negative, SM = small, LN = large negative) as with five membership functions.

The next step in the design of the fuzzy "engine" involves the definition of the inference rules for the fusion of the MRI and PET wavelet coefficients. Nine rules comprised of conditional if-then statements are determined for the system with 3 membership functions. These rules are displayed in Figure 3.8. The method that defines the fuzzy operator AND, which is utilized in the determination of the inference rules, is set to "min."

The next subsection of this chapter provides an outline of the steps for the implementation of the hybrid fuzzy-wavelet fusion system with the parameters presented above.

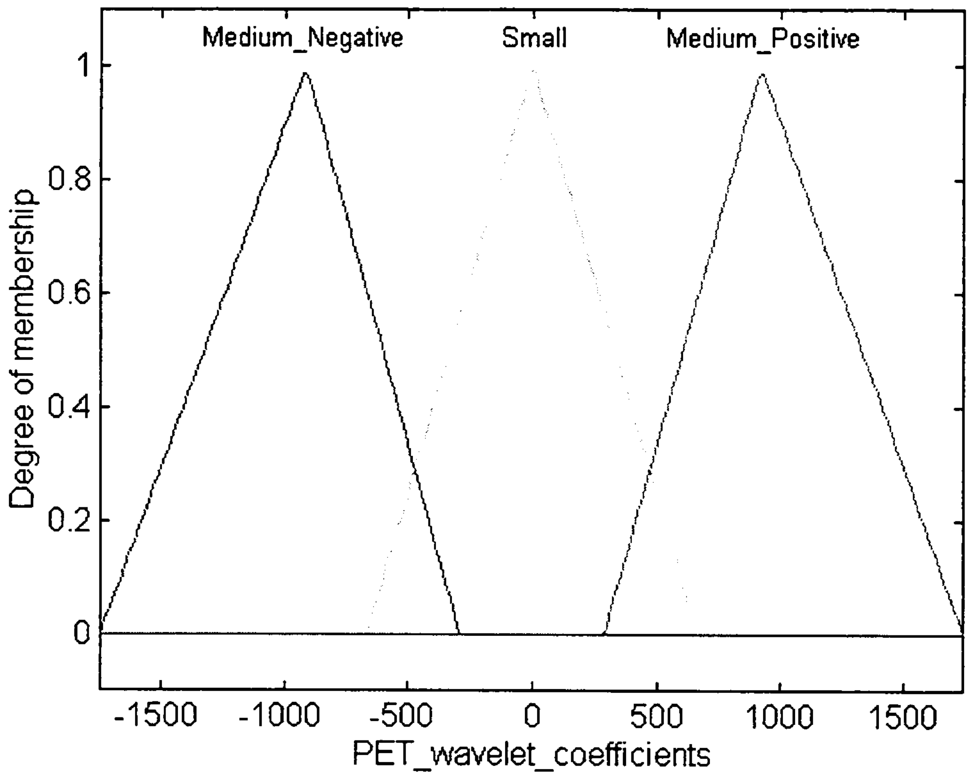

Figure 3.7. Final membership function design associated with the input and output variables.

1. If (PET_wavelet_coefficients is Medium_Negative) and (MRI_wavelet_coefficients is Medium_Negative) then (Fused_wavelet_coefficients is Medium_Negative) (1)

2. If (PET_wavelet_coefficients is Medium_Negative) and (MRI_wavelet_coefficients is Small) then (Fused_wavelet_coefficients is Medium_Negative) (1)

3. If (PET_wavelet_coefficients is Medium_Negative) and (MRI_wavelet_coefficients is Medium_Positive) then (Fused_wavelet_coefficients is Medium_Positive) (1)

4. If (PET_wavelet_coefficients is Small) and (MRI_wavelet_coefficients is Medium_Negative) then (Fused_wavelet_coefficients is Medium_Negative) (1)

5. If (PET_wavelet_coefficients is Small) and (MRI_wavelet_coefficients is Small) then (Fused_wavelet_coefficients is Small) (1)

6. If (PET_wavelet_coefficients is Small) and (MRI_wavelet_coefficients is Medium_Positive) then (Fused_wavelet_coefficients is Medium_Positive) (1)

7. If (PET_wavelet_coefficients is Medium_Positive) and (MRI_wavelet_coefficients is Medium_Negative) then (Fused_wavelet_coefficients is Medium_Positive) (1)

8. If (PET_wavelet_coefficients is Medium_Positive) and (MRI_wavelet_coefficients is Small) then (Fused_wavelet_coefficients is Medium_Positive) (1)

9. If (PET_wavelet_coefficients is Medium_Positive) and (MRI_wavelet_coefficients is Medium_Positive) then (Fused_wavelet_coefficients is Medium_Positive) (1)

Figure 3.8. Rules defined for the fuzzy-wavelet system with 3 membership functions

3.2.4 Hybrid Fuzzy-Wavelet Fusion Implementation

Wavelet toolbox functions gathered in a batch program, associated with a fuzzy inference system, constitute the basis for the proposed hybrid fuzzy-wavelet method. The methodology defined for the fusion of the medical image sets used in this work may be summarized in the following steps, as described in Appendix A, Program 2:

1. The coregistered PET and MRI images are loaded into MATLAB. A synthetic image filled with zeros, which will later store the data structure of the fused image, is created and loaded at this stage;
2. A biorthogonal 3.7 (bior 3.7) basis function is selected to perform a 2-D wavelet packet decomposition of the loaded images in 2 levels. The wavelet packet tree structure of these images is similar to the one displayed in Figure 3.4;
3. A wavelet tree structure (similar to Figure 3.5) is obtained by the recomposition of the nodes that represent the matrices of detail coefficients in the first decomposition level. The structure that contains the data is automatically updated;
4. All matrices of detail and of approximation coefficients of each image are read and stored in separate matrices for further processing;
5. The boundaries of the matrix of approximation coefficients at the second level of decomposition are normalized for an enhancement of image features. The normalization factor is defined as:

max(abs(MRI wavelet coefficients)) / max(abs(PET wavelet coefficients));

6. The fuzzy inference system (FIS) described in Appendix A, Program 6 is called to perform the fusion of the matrix of wavelet approximation coefficients obtained at the second level of decomposition. As explained in Section 3.3.1, image fusion with the methodology being presented only requires the combination of the PET and MRI wavelet approximation coefficients, since they fully characterize the relevant image features without the need of additional information from the matrices of detail coefficients;
7. An optional feature available at this stage consists of further enhancing the anatomical and functional image features in the fused output image by simply increasing the active range of the universe of discourse of the inputs and output in the fuzzy system. This improvement may also be accomplished by modifying the width of occupancy of selected membership functions in the fuzzy system;
8. The fused wavelet coefficient matrix is stored in the data structure of the synthethic image, which is then reconstructed with the inverse wavelet packet transform, in order to obtain the resultant fused output image;
9. The fused output image is displayed for visual evaluation.

CHAPTER 4

RESULTS

4.1 Data Description

There are three sets of images that have been used for the validation and testing of the different algorithms implemented in this thesis. These sets consist of registered MRI and PET brain images. While a large number of sources of medical images may be found on the INTERNET, the task of locating registered sets from the same patient proved to be a more difficult one. Registration remains a fairly elaborate procedure only performed under special circumstances of research or diagnostic interest, not usually constituting a routine image processing task in hospitals or medical research institutions. A short description of the image sets used in this investigation follows, as well as the abbreviated clinical diagnosis pertaining to them.

Set 1.

This image set was obtained from the Department of Radiology of the University of Tennessee Medical Center at Knoxville, TN, USA [50]. The patient was submitted to MRI and PET studies on the same day, and was diagnosed with a brain tumor. Figure 4.1 shows the MRI image which corresponds to slice number 12 on a series of 19 acquired axial T-3 weighted MRI scans. It is a 256 x 256 image with thickness of 5 mm and pixel size of 0.94 mm, stored in 8 bits per pixel.

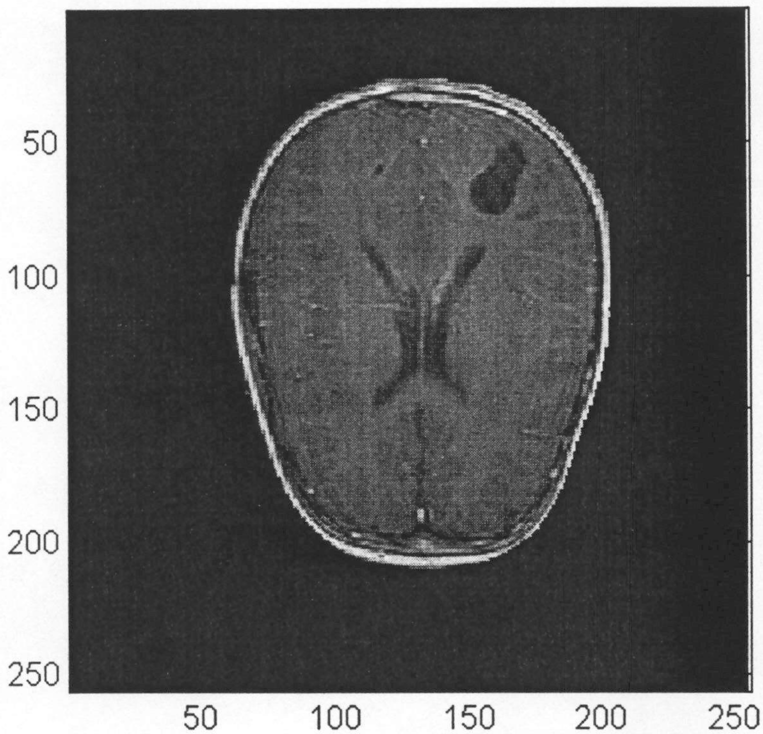

Figure 4.1. MRI image [50].

Figure 4.2 depicts slice number 20 of a series of 47 axial PET emission images, zoomed to a size of 256 x 256 from the original 128 x 128 PET slice, with a pixel size of 1.05 mm, stored in 8 bits per pixel. It should be noted here that these image sets have not been registered, and are therefore utilized only to aid in the testing and illustration of preprocessing techniques applied in this work.

Set 2.

This group of images was obtained from the " Whole Brain Atlas", an information resource for central nervous system imaging at Harvard Medical School [51]. A set of PET and MRI scans that exemplifies a brain tumor occurrence was chosen. This set of images corresponds to a case in which the patient, who had been previously treated with whole brain radiation therapy due to an astrocytoma, was resubmitted to MRI and PET studies because of prompt seizure recurrence after attempts to wean the steroid treatment. The PET scan efficiently helped distinguish tumor recurrence from radiation necrosis here, by showing a high metabolic activity in the same region of the previously treated tumor.

Figure 4.3 depicts the 256 x 256 axial MRI scan corresponding to slice 60 of the 125-image study, while Figure 4.4 shows the 256 x 256 coregistered PET scan. Both scans are stored in 8 bits per pixel. It should be noted that Figures 4.3 and 4.4 have been preprocessed prior to their inclusion in the web site, and are therefore utilized only for the implementation of the fuzzy-wavelet fusion scheme.

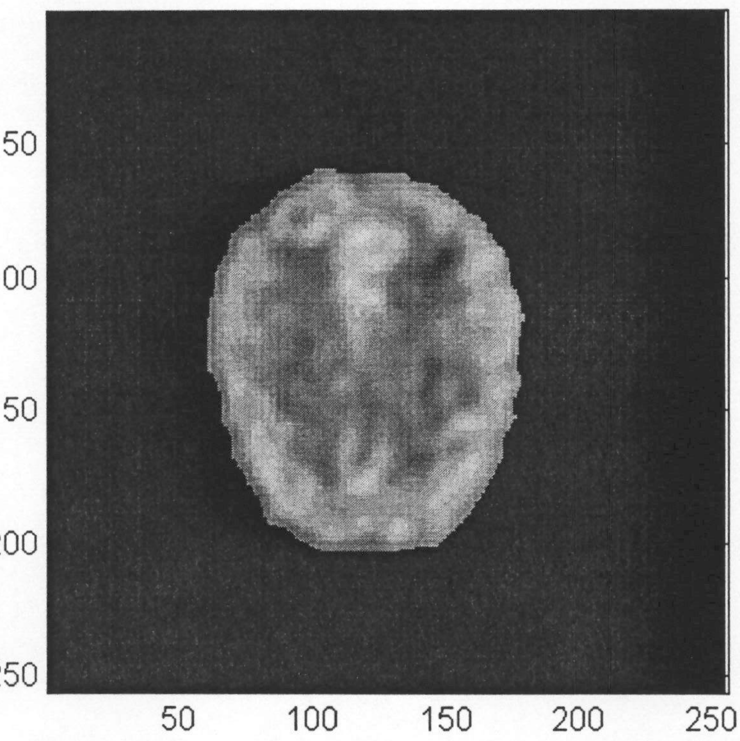

Figure 4.2. PET image [50].

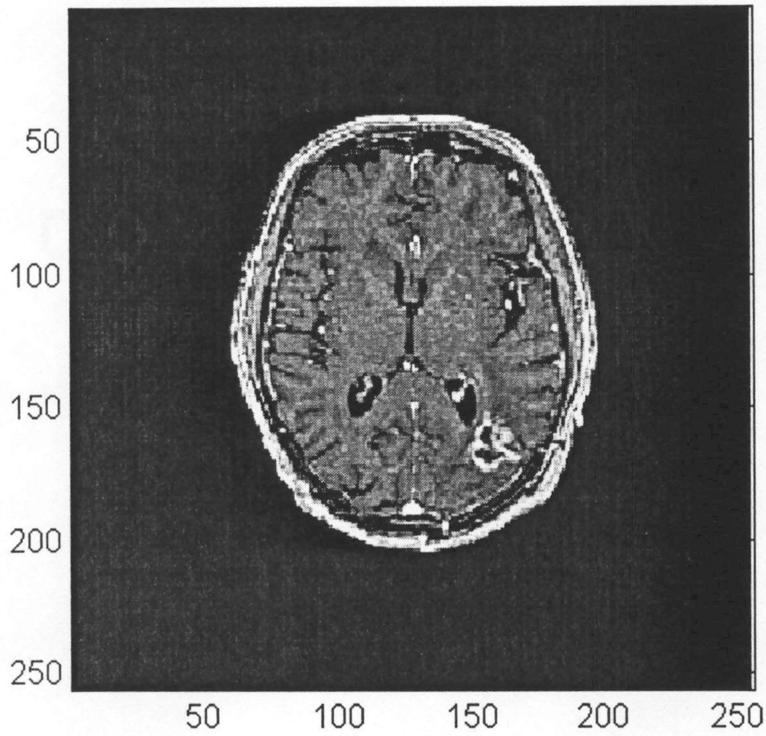

Figure 4.3. MRI image [51].

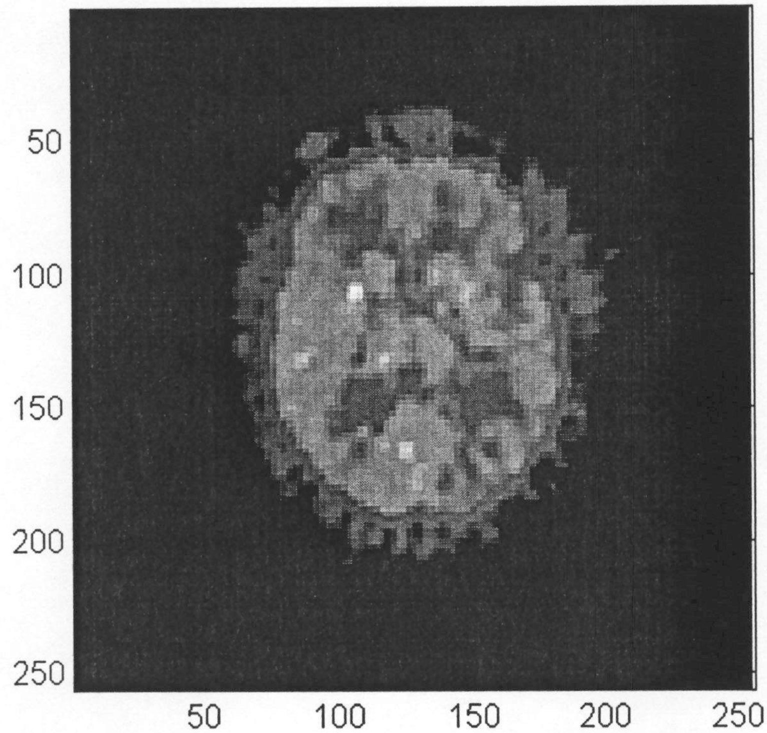

Figure 4.4. PET image [51].

Set 3.

The images in this set were obtained from the Laboratory of Functional and Multidimensional Imaging of the Geneva University Hospitals, Geneva, Switzerland [52]. The data are from an epileptic patient, and the images were produced in the scope of a pre-surgical investigation. Pathology is diffused in this case, and is well characterized through metabolic information from PET and SPECT. The scans reveal the extent of the concerned area; cortical grid and strips are then surgically implanted to correlate the findings with electrophysiology data directly at the level of the cortex [52].

Figure 4.5 depicts the sagittal 256 x 256 MRI scan and Figure 4.6 shows the 256 x 256 coregistered PET scan, both of which are stored in 8 bits per pixel. These scans are also utilized to test the fuzzy-wavelet implementation presented here.

4.2 Image Fusion Results

The implementation described in this thesis is an innovative combination of two different technologies geared specifically towards the improvement and optimization of the fusion task in the field of medical image analysis. Therefore, the analysis provided here exposes an introductory evaluation of many parameters that influence the hybrid system. It also outlines the basic implementation steps to be followed in a more detailed and in-depth investigation of the contribution of each of these parameters to the performance of the system.

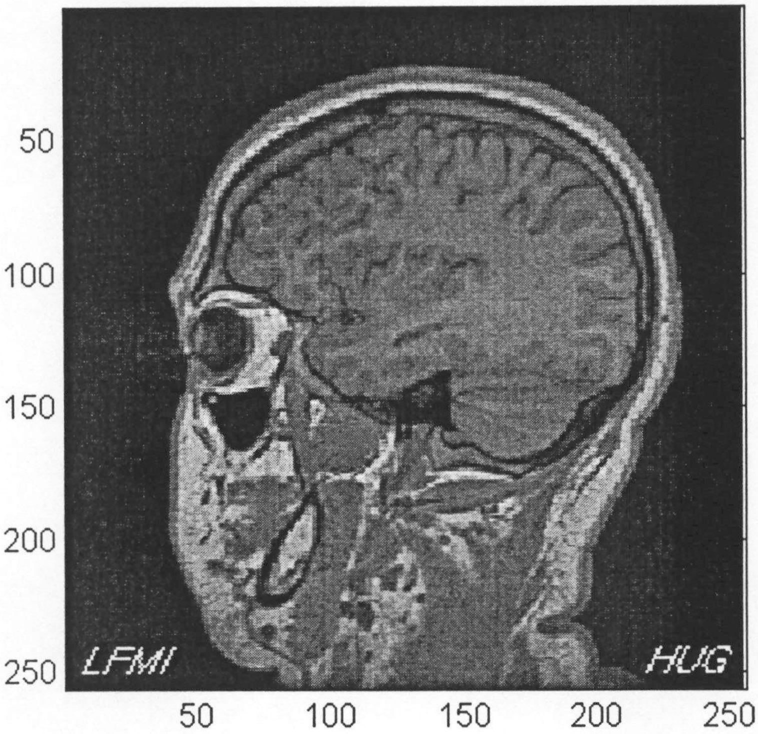

Figure 4.5. MRI image [52].

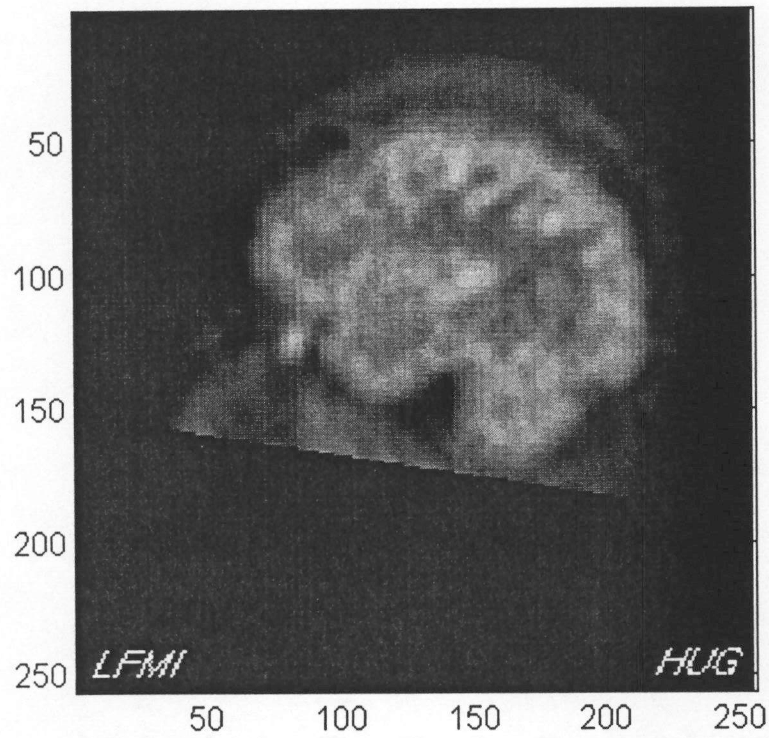

Figure 4.6. PET image [52].

First, the outcome of the selection of the most adequate wavelet basis function for the fusion task is shown, followed by an exposition of results obtained with the classical wavelet fusion technique. Then, results obtained by varying relevant system parameters in the hybrid method are presented. All implementation phases and details regarding decisions about the variation of parameters are discussed in the implementation section of the thesis (Chapter 3).

4.2.1 Optimal Wavelet Selection for Fusion

Choosing an adequate wavelet basis function is fundamental for the accurate representation of the signal or image to be analyzed. The closer the wavelet prototype function is able to describe the singularities of the actual 2-D signal, the more precise is the reconstruction of the image by the wavelet transform. A discussion on the specific characteristics of the wavelet prototype functions utilized in image analysis has been given in Chapter 3, where it was cited that the Daubechies and biorthogonal wavelet bases are most widely used in the current literature for image processing tasks.

Figures 4.7a-c depict a fused image (MRI image in Figure 4.3 and PET image in Figure 4.4 fused by the fuzzy-wavelet approach) processed with a Daubechies basis function with three different vanishing moments, namely Daubechies 2, 12, and 20 respectively.

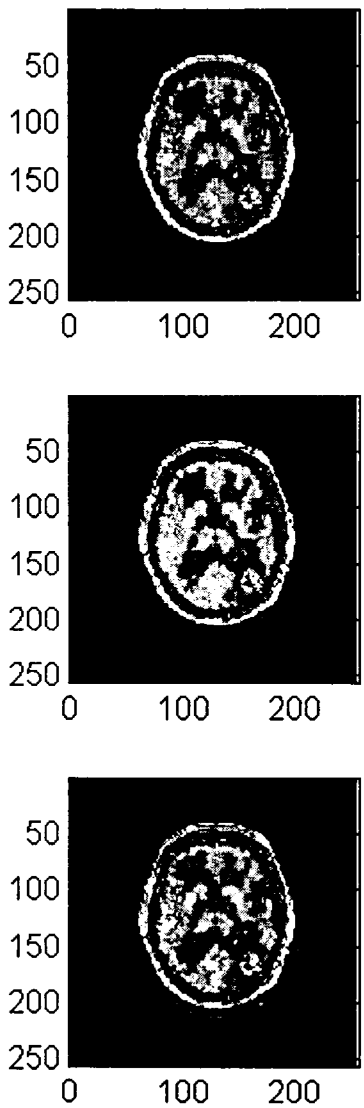

Figure 4.7. Fused image with Daubechies wavelets. (a) Daubechies 2, (b) Daubechies 12, (c) Daubechies 20.

Figures 4.8a-c show the same fused image processed with a biorthogonal basis function with three distinct vanishing moments, namely biorthogonal 2.2, 3.7, and 6.8. The results provided in Figures 4.7 and 4.8 show that, while any of the biorthogonal prototype functions accurately portrays the fusion, the Daubechies basis functions with higher order of vanishing moments produce image artifacts similar to "rings" at the outer border of the image. The higher the order of the vanishing moment, the more pronounced are the rings, although the information content of the image is adequately represented.

The artifacts seen in Figure 4.7 are due to border distortions caused as the result of the shape of the prototype function used. The number of vanishing moments characterizes the number of oscillations inherent in the shape of the basis function that is used to analyze the image. Therefore, when a prototype function with higher vanishing moments is selected, more oscillations are introduced in the representation of the border, and more artifacts are generated. These artifacts may be reduced by performing a polynomial extrapolation of the 2-D signal at the boundaries.

It is also apparent from Figure 4.7 that the image fused with the Daubechies 2 basis function presents a certain degree of "blockyness" in the representation of its features, while the Daubechies 12 and 20 provide smoother representations of the image content. After a careful review of the results presented above, the biorthogonal prototype functions are found to be very appropriate for the fusion task.

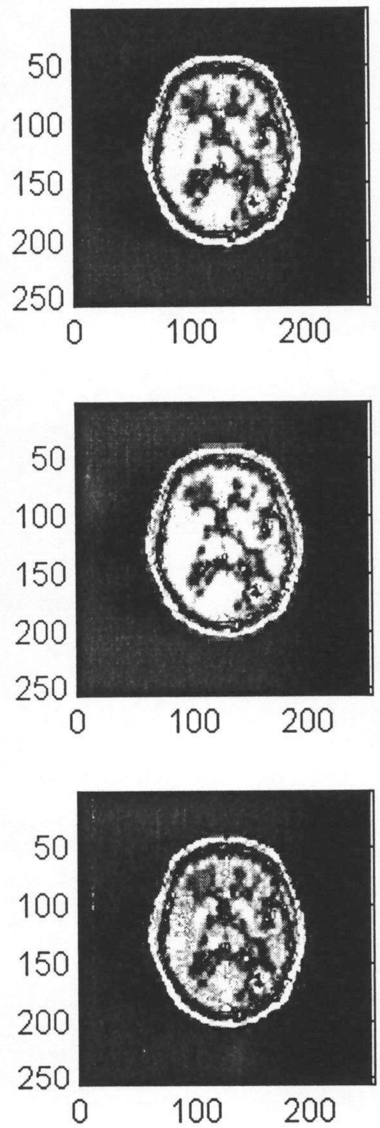

Figure 4.8. Fused image with biorthogonal wavelets. (a) biorthogonal 2.2,

(b) biorthogonal 3.7, (c) biorthogonal 6.8.

The Daubechies 12 basis function is also suitable, in spite of the boundary effect problems. These problems may be easily overcome by signal extension at the boundaries, as explained earlier. In general, prototype functions with lower order of vanishing moments are found to be more appropriate to the fusion of the medical images analyzed in this thesis, since the information content of these images is well characterized in the lower frequency levels. Therefore, the biorthogonal 3.7 is the basis function of choice for the illustration of the analysis and performance of the fuzzy-wavelet fusion approach in this thesis.

4.2.2 Classical Wavelet Fusion Results

As described in previous chapters, the key to the successful application of wavelet processing in such a variety of fields is the clever manipulation of the wavelet coefficients so as to obtain the desired output in the reconstructed signal or image. In the particular case of image fusion, the main focus is on selecting a rule for the integration of these wavelet coefficients. The classical method proposes the selection of the coefficients whose absolute values are higher at every point in the transform domain ("max" rule), since large coefficients indicate sharper brightness changes that characterize edges or salient features in the image. The implementation of this "max" rule was discussed in detail in Chapter 3, and constitutes the method utilized in obtaining the results reported here.

Figure 4.9 depicts the fusion of the images in Set 2 at the third level of decomposition with a biorthogonal 3.7 basis function. Figure 4.9a is obtained by integrating all matrices of wavelet coefficients at all three levels of decomposition with the "max" rule. Figure 4.8b is obtained by utilizing the same method, except that the approximation coefficients at decomposition level 3 are multiplied by a normalization or enhancement factor as outlined in Chapter 3.

Figure 4.10 portrays the fusion of the PET and MRI scans in Set 3. As in the previous case, Figure 4.10a depicts the fusion by the "max" rule without enhancement, while Figure 4.10b portrays the same fusion method with the addition of the enhancement component. The results in both figures indicate that the fusion by the "max" rule is indeed a very efficient procedure, since anatomical and functional features are well blended and recognizable in the output image. The enhanced fused images are excellent in their portrayal of the functional content from the PET scans, allowing for a more accurate anatomical localization of the extent of the pathology or condition revealed by the functional PET information.

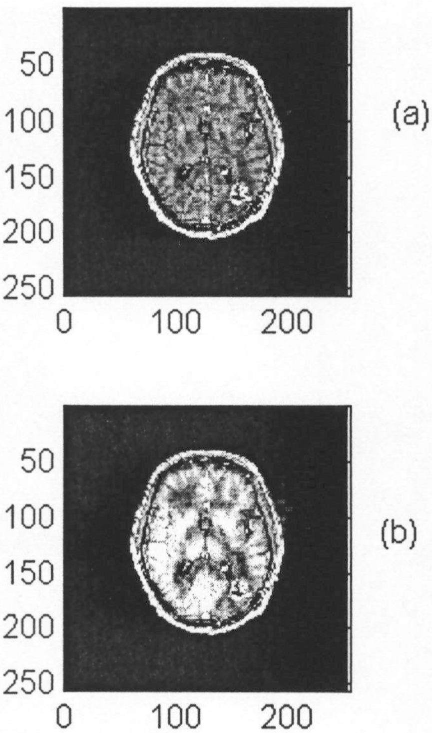

Figure 4.9. Classical image fusion [51]. (a) Without enhancement, (b) Enhanced.

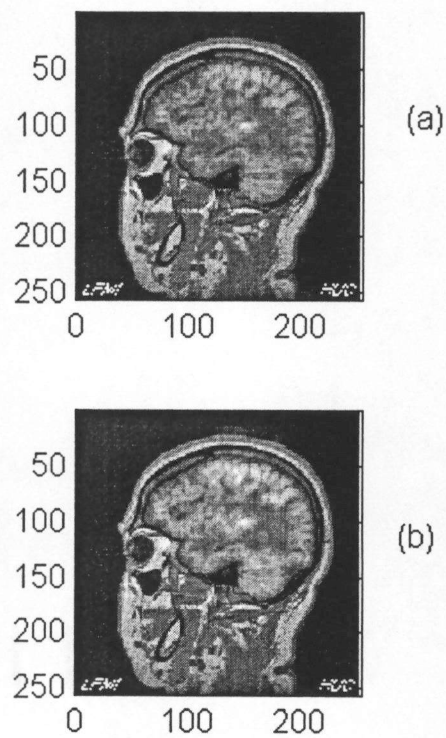

Figure 4.10. Classical image fusion [52]. (a) Without enhancement, (b) Enhanced.

4.2.3 Hybrid Fuzzy-Wavelet Fusion Results

The hybrid fusion method introduced in this thesis incorporates the versatility of selecting and combining wavelet coefficients that portray relevant information at specific resolution levels with the flexibility of designing fusion rules that model the inherent degree of fuzziness of the medical image data by fuzzy logic. Due to the intrinsic adaptability of both techniques, many parameters need to be varied and evaluated in the search for the most adequate representation of the fusion process. The results presented here are divided in sections that show how these different parameters may be varied and how they are combined to produce the desired fused output image. First, the optimal level for the decomposition of the images by the wavelet transform is investigated, followed by the exposition of results obtained by varying the design of the fuzzy inference system in terms of the number of membership functions and rules that implement the actual fusion scheme. Furthermore, an exemplification on how the hybrid fusion system may be utilized for the simultaneous fusion and enhancement of image features is also presented. Details on the procedure for varying the different parameters in the fuzzy-wavelet fusion scheme and on the significance of these variations are provided in the implementation section, Chapter 3, of this thesis.

4.2.3.1 Selection of the Wavelet Decomposition Level

Theoretically, the limit of the level of decomposition (j) of the image with the wavelet transform is imposed by the size of the image on the dyadic scale 2^j, where j is an integer defined on the interval $[1,2,....,\log_2 N]$, with N representing the size of the image. In practice, however, the wavelet decomposition level selected for the specific purpose of image analysis corresponds to the level at which the desired image features are best represented. Figures 4.11a-c show the fusion of the images in set 2 with a biorthogonal 3.7 wavelet basis function at decomposition levels 2, 3, and 4 respectively.

The fused image at level 2 depicts a well-balanced combination of anatomical features from the MRI and functional information from the PET. As the level of decomposition increases, less features from the image characterized by lower frequency components and poorer spatial resolution (PET scan in this case) are present in the fused output image. Since the MRI scan presents more details (better image definition) than the PET in the matrix of wavelet approximation coefficients, it looses information content at a slower rate then the PET upon successive wavelet decompositions. The images in Figures 4.11b-c adequately illustrate this fact, with the image in Figure 4.11c portraying very little functional PET information when compared to the images in Figures 4.11 a-b .

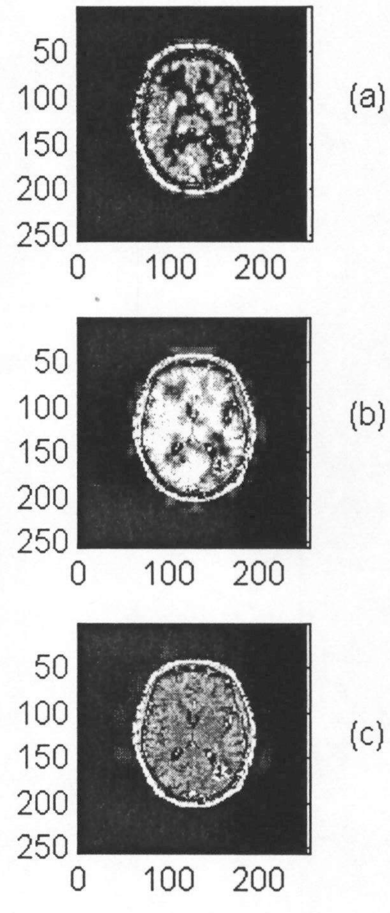

Figure 4.11. Fusion at different decomposition levels [51]. (a) level 2, (b) level 3, (c) level 4.

Therefore, in order to obtain an output fused image which accurately represents both function and anatomy of the region being imaged, level 2 is selected as the level of wavelet decomposition best suited for the fusion of the specific sets of head scans. It should be noted that the level of wavelet decomposition selected for fusion is always dependent on the type of images to be evaluated and on the manner in which the relevant information is portrayed in such images.Figure 4.12 shows the outcome of the fuzzy-wavelet fusion scheme applied to the images in Set 3 at the second level of wavelet decomposition. This image efficiently characterizes the correspondence between the anatomical and functional information from the original MRI and PET source images.

4.2.3.2 Fuzzy Inference System Design Results

As described in Chapter 3, the design of an effective Fuzzy Inference System (FIS) for fusion of multimodality images requires great knowledge of the nature of the data being analyzed. The parameters that affect the design of this system have been discussed in detail in the previous chapter, and the two different "fuzzy engines" utilized are shown in Figures 3.6-3.7. The first FIS with 5 triangular membership functions and 25 fusion rules is utilized in conjunction with the wavelet transform to obtain the fusion of the images in Set 2, as seen in Figure 4.13a. The same fuzzy-wavelet system is also used to fuse the images in Set 3, and the result is shown in Figure 4.14a.

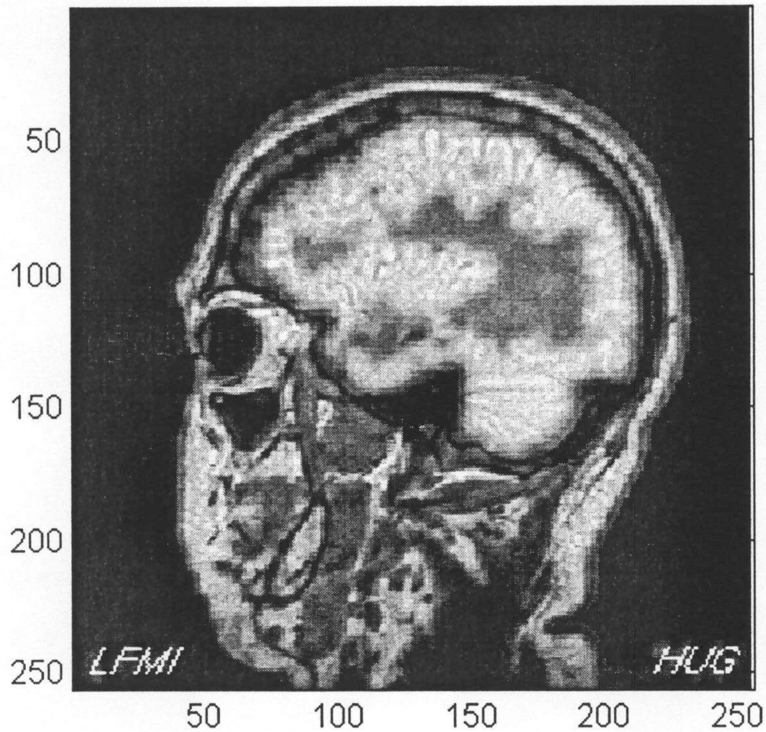

Figure 4.12. Fusion at decomposition level 2 [52].

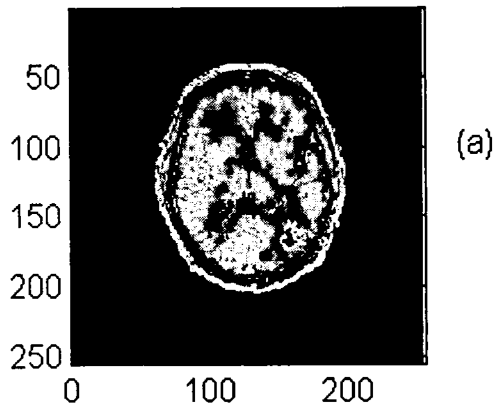

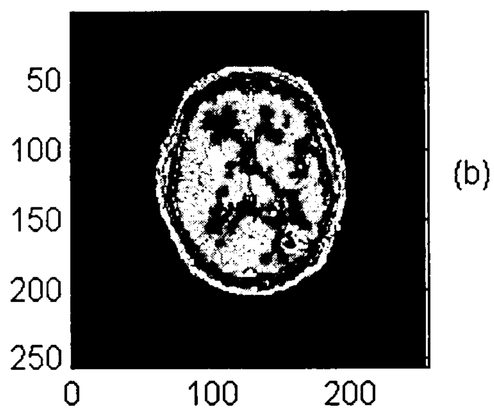

Figure 4.13. Fusion with different FIS designs [51]. (a) 5 membership functions, (b) 3 membership functions.

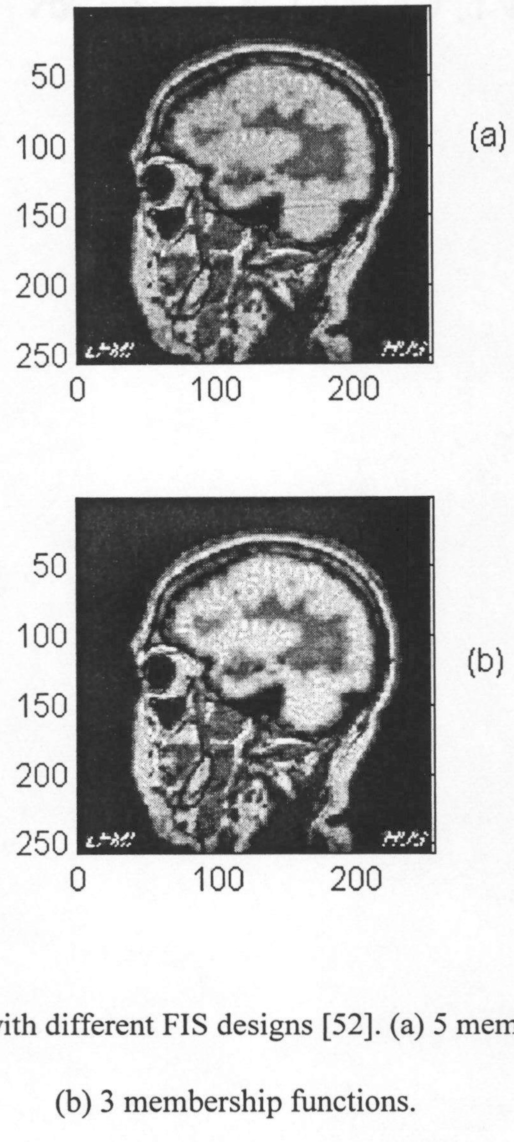

Figure 4.14. Fusion with different FIS designs [52]. (a) 5 membership functions, (b) 3 membership functions.

A second FIS design consisting of 3 triangular membership functions with 9 specified fusion rules is successfully applied to the images in set 2 and 3, and the results are portrayed in Figures 4.13b and 4.14b respectively.

It was our expectation that a FIS with a higher number of both membership functions and rules would produce a fused image with more accurately defined details and more distinguishable features. Nonetheless, as Figures 4.13 and 4.14 show, increasing the number of membership functions and rules does not provide a relevant improvement in the image definition. This is likely due to the inherent nature of the image data being analyzed, such as the intrinsic fuzzyness of the PET image. Due to the results obtained here, the FIS design that consists of 3 membership functions and 9 rules is selected as the best choice for our implementation, since fewer rules are fired in the processing of the data with this FIS, and less computational effort is needed for the completion of the analysis in less time.

4.2.3.3 Enhancement Factor Selection Results

One of the great advantages of the fuzzy-wavelet fusion approach proposed in this work is the possibility of enhancing selected image features by modifying the width of occupancy of specific membership functions or by increasing the active range of the universe of discourse. This enhancement is performed simultaneously with the fusion without the burden of additional programming or computations. Figure 4.15c exemplifies the above mentioned form of enhancement applied with the fusion of images in Set 2, while Figure 4.16c shows its application with the fusion of the images in Set 3.

Another contrast improvement factor involving the normalization of the range of the matrix of wavelet coefficients is also implemented here. Since the range of the wavelet approximation coefficients of the PET images is usually smaller than the range of the corresponding MRI coefficients, a multiplication factor is applied to the PET wavelet coefficients so that both PET and MRI coefficients have the same boundary values prior to the fusion with the FIS. The results obtained by applying this specific enhancement procedure to image sets 2 and 3 are portrayed in Figures 4.15b and 4.16b respectively. The fused image of Set 2 is shown without any enhancement in Figure 4.15a; Figures 4.15b-c show how both enhancement factors applied with the fuzzy-wavelet scheme greatly improve the contrast of the different anatomical and functional features in the fused image. Similar results are portrayed in Figures 4.16a-c for the images in Set 3.

The results presented in this chapter provide an introductory evaluation of the potential of the proposed fuzzy-wavelet fusion technique in the analysis of medical images. Although the parameters that characterize the system need to be further researched for an optimal system implementation, the preliminary results demonstrate that the method is a successful and feasible alternative to the classical wavelet fusion procedure.

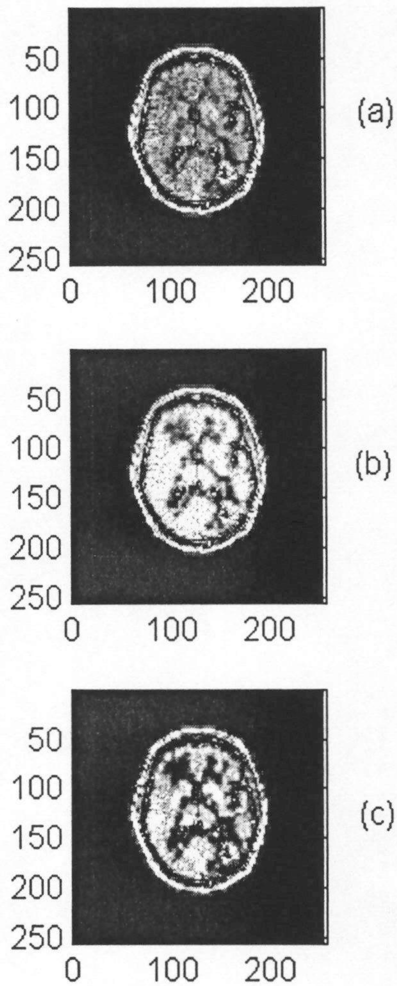

Figure 4.15. Image fusion with different enhancement factors [51]. (a) no enhancement, (b) enhancement with a multiplication factor, (c) enhancement with a change in the universe of discourse.

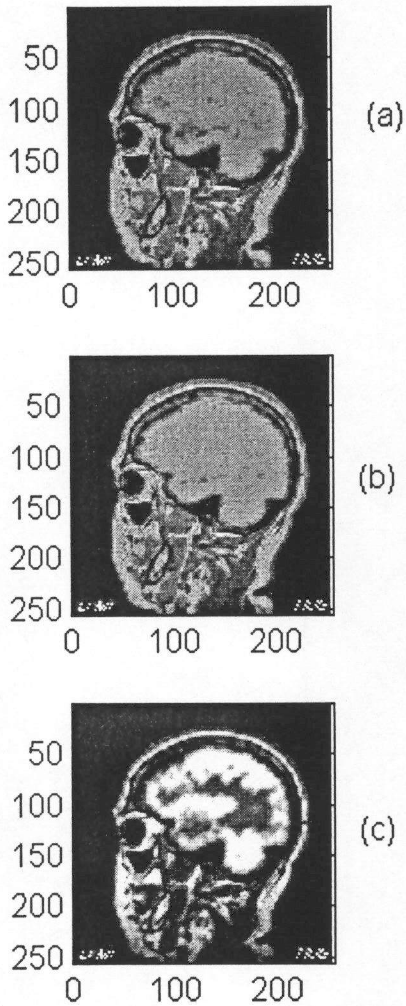

Figure 4.16. Image fusion with different enhancement factors [52]. (a) no enhancement, (b) enhancement with a multiplication factor, (c) enhancement with a change in the universe of discourse.

The scheme provides for an incredible versatility in the combination of the wavelet coefficients for selective feature modeling; it allows a flexible implementation of membership functions and rules that determine the fusion of ill-defined data. It also permits the simultaneous enhancement of the images with the fusion process.

Furthermore, the fusion is performed by utilizing only the matrix of approximation wavelet coefficients at the desired decomposition level with remarkable effectiveness. This allows for noise removal, since the detail wavelet coefficients which characterize higher frequency components (noise) are not included in the actual fusion procedure.

Figure 4.17 provides a means of comparison between the efficacy of the classical wavelet fusion approach and that of the hybrid fuzzy-wavelet method. Both schemes are applied to the fusion of the images in Set 2 by utilizing only the matrix of wavelet approximation coefficients at the second level of decomposition. Figure 4.17 reveals that, while the classical method produces poor fusion results in terms of resolution and image content definition of the fused output, the fuzzy-wavelet method excels in the representation of the fused image, with excellent portrayal of both anatomical and functional details from the respective MRI and PET scans. The visual difference in the output fused images in Figure 4.17 is impressive, and constitutes an advantage of the hybrid method that prompts further investigation in the optimization of the system.

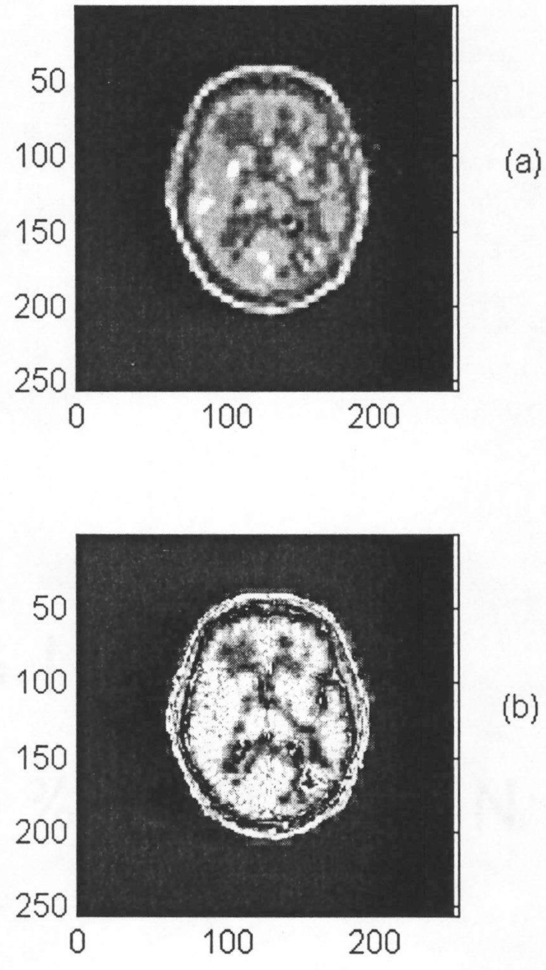

Figure 4.17. Comparison between results from the two different image fusion techniques [51]. (a) classical fusion result, (b) hybrid fuzzy-wavelet result.

CHAPTER 5

AUXILIARY APPLICATIONS

5.1 Introduction

As mentioned in the System Implementation Chapter of this thesis, medical images generally require some form of preprocessing prior to the assessment of their characteristics and thorough analysis of their features. This requirement is due to a number of difficulties imposed by the process of acquiring images of living organisms, as well as limitations dictated by the equipment and imaging acquisition methods utilized [53]. The preprocessing component of the system illustrated in Figures 3.1 and 3.2 comprises different algorithms that may be applied to the improvement of images prior to their fusion. This preprocessing stage is treated as an auxiliary or secondary system in the fusion process, and its implementation is the topic of discussion in this chapter. Results obtained with a few classical image preprocessing methods are compared to those achieved with wavelet transforms. These results are presented at the end of the chapter.

5.2 Preprocessing System Implementation

The analysis of medical images requires a considerable effort in the adequate preparation of the images for further processing. Images acquired with different techniques need to be reformatted to a common representation form. Reformatting may include a change in the original image coordinate system or a modification in the image orientation. Images often need to be edited (cropped for the removal of unnecessary information and padded for restoring to their size prior to the crop), interpolated or zoomed, and then aligned, as in the case of multimodality image analysis.

In order to perform fusion, it is absolutely crucial that the different images be aligned or matched to a near pixel level. This complex procedure is known as registration, and constitutes an unavoidable preprocessing step for the fusion of medical images. Several registration methods are discussed in detail in [1,2,30], but one of the most efficient and complete packages that specifically targets the registration of medical images is the Automatic Image Registration (AIR 3.0) software developed by Roger Woods of the UCLA School of Medicine [48]. The implementation of a coregistration scheme is, however, beyond the scope of this thesis. All images utilized in the fuzzy-wavelet scheme proposed in this work have been previously registered.

In general, preprocessing of images beyond registration includes noise removal, contrast enhancement, segmentation, edge detection, feature classification, among others. In the development of the present methodology, only noise removal and image enhancement are implemented, since these techniques effectively enhance features related to the fusion of images.

The improvement of images through the removal of noise and enhancement of constituent features is based on statistical analysis. In classical methods, image histograms are computed and their characteristic components (modes) analyzed in terms of statistical moments (mean, variance, or higher-order statistics). This is performed for the adequate selection of a threshold for the elimination of noise or for the selection of regions and image features to be enhanced. On the other hand, denoising and contrast improvement via wavelets is achieved by thresholding of the wavelet coefficients. These coefficients are obtained by applying a wavelet transform to the image. In denoising, the wavelet coefficients that represent noise (sharp gray-level transitions) are removed, and the remaining coefficients provide better estimates of the relevant image content. Many wavelet denoising methods were developed with special thresholding techniques, as cited in [55,57]. Interested readers are directed to references [7,49,55-59] for a detailed discussion on statistical analysis for denoising and enhancement of signals and images with classical and wavelet-based methods.

5.2.1 Noise Removal Methodology

Medical images may often present structured or random noise. The following procedure outlines the steps for the removal of structured noise from images:

1. The automatic threshold selection procedure developed by Ostu in [49] is used to remove the background noise of a selected head image. The code for this algorithm is included in Appendix A, Program 3;

2. The outline or boundary of the head in the image is computed. The algorithm is specified in Appendix A, Program 4;
3. The original noisy head image and the outline of the head are used to reconstruct the relevant image content lost in the processing of Step 1. The output image is a denoised version of the original with all relevant information intact. The corresponding code is given in Appendix A, Program 5.

In order to illustrate the removal of random noise in an adequate manner, we synthetically add a considerable amount of this type of noise to an image. Denoising is accomplished through the following method:

1. A Daubechies 2 prototype function is selected in the wavelet toolbox for the decomposition of the image in three resolution levels by means of the wavelet framework. The automatic threshold option is chosen for the denoising, and the output is obtained with the MATLAB Graphic User Interface (GUI);
2. The wavelet packet framework is used by selecting a Daubechies 2 prototype function in the wavelet toolbox for the decomposition of the image in three resolution levels. The SURE entropy parameter [42] is chosen, and the optimal denoising is performed by analyzing the image with different global thresholds selected in the GUI. A global threshold of 24 is found to provide the best denoised output image;

3. A comparison between the wavelet and the wavelet packet frameworks for the removal of random noise is drawn, and the result is reported in a subsequent section of this chapter.

It should be noted that the SURE entropy parameter mentioned above in Step 2 refers to a threshold selection rule based on Stein's Unbiased Risk Estimate (quadratic loss function) that may be utilized for denoising with the wavelet packet analysis. Details on this threshold estimator function may be found in [42, 55, 57].

5.2.2 Contrast Enhancement Methodology

Another preprocessing method which constitutes a part of this methodology is contrast enhancement. Among numerous procedures for image improvement from a variety of fields, a popular filtering technique and the wavelet transform are chosen here to illustrate the implementation of this enhancement task. A classical filtering method known as the "unsharp" filter provides the removal of lower frequency components from the image by subtracting its blurred version from the original, causing an improvement in the identification of features [7]. It should be noted that contrast enhancement and noise filtering are many times achieved through the same procedure, that is, removing noise from a medical image may also bring out important diagnostic features. The noise removal process with the "unsharp" filter is implemented with a function available in MATLAB. In the MATLAB Image toolbox, the "unsharp" filter option is chosen, which automatically implements a 3 x 3 contrast enhancement filter that is applied to the chosen image. The result is discussed later in this chapter. The wavelet technique as applied to the improvement of image contrast is described in the following steps:

1. A wavelet packet decomposition of the chosen image in two levels with a Daubechies 2 basis function is performed. The corresponding code is listed in Appendix A, Program 6;
2. Upon the wavelet packet decomposition, only the matrix of approximation coefficients at the second level, multiplied by a factor of 2, is utilized for the reconstruction of the image;
3. The resulting enhanced image is displayed for evaluation, and the result presented later in this chapter.

By ignoring all detail coefficient matrices in the wavelet packet reconstruction of the image, we bring out image features characterized by wavelet packet coefficients that correspond to signal averages in the original 2-D image. Selectively multiplying certain groups of wavelet packet approximation coefficients that fall under user-defined criteria by a factor(s) promotes additional local enhancement of features described by them. A comparison of the two different enhancement methods described here is done in the results section of this chapter.

5.3 Preprocessing System Results

The results below illustrate the suitability of a few widely documented traditional procedures and of wavelet techniques to some image preprocessing tasks. This preprocessing is usually performed prior to image registration and fusion. While it is beyond the scope of this project to provide a review of preprocessing techniques for medical image analysis, a simple illustration of the power of the wavelet technique in this area further emphasizes its versatility and supports its utilization in the implementation of an image fusion scheme.

5.3.1 Noise Removal

This section illustrates the removal of two types of noise that may affect medical images, namely structured and random noise. The automatic threshold selection procedure suggested in reference [49] is applied to the PET image in Figure 5.1, which depicts some inherent structured noise. The result conveyed in Figure 5.2 reveals that, while the algorithm accomplished the total extraction of the background noise, it also caused the removal of relevant functional information from within the image. In order to overcome this adverse effect, the corresponding contour or outline image of Figure 5.3 is utilized in conjunction with the original PET image of Figure 5.1 as explained in Section 5.2.1 to obtain the image in Figure 5.4. Figure 5.4 reflects the desired output: a denoised PET image with all relevant image information intact.

The existence of random noise in medical images is directly related to the density of information represented in these images [54]. The wavelet approach has proven to be very effective in the removal of noise from different image modalities. Figures 5.5a-b

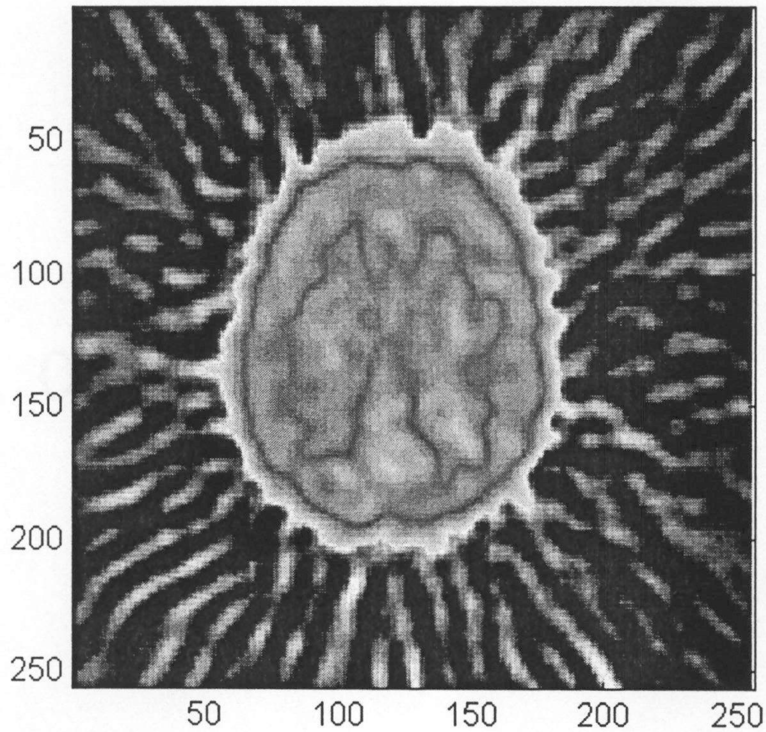

Figure 5.1. Noisy PET scan [50].

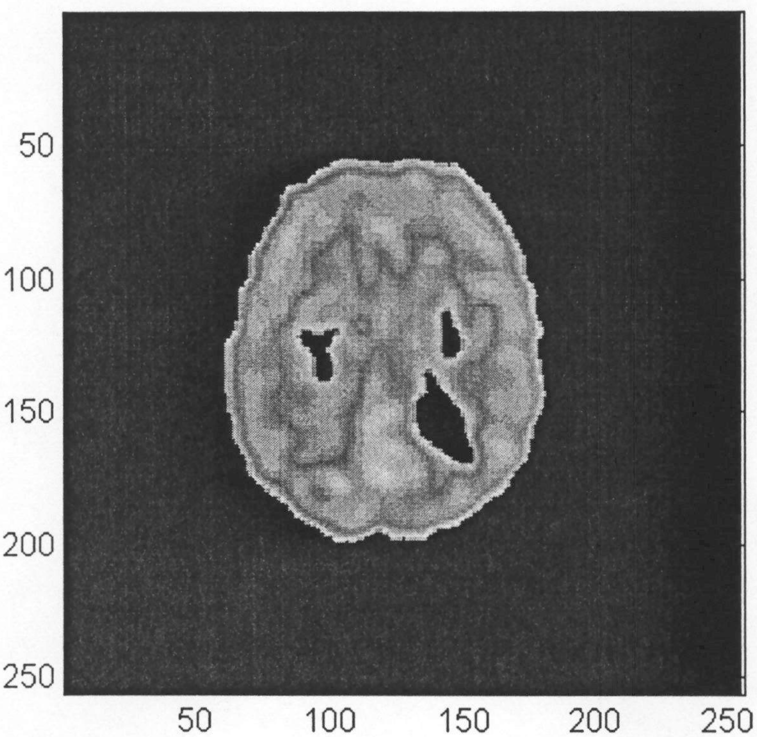

Figure 5.2. PET scan after thresholding with Otsu's algorithm [49,50].

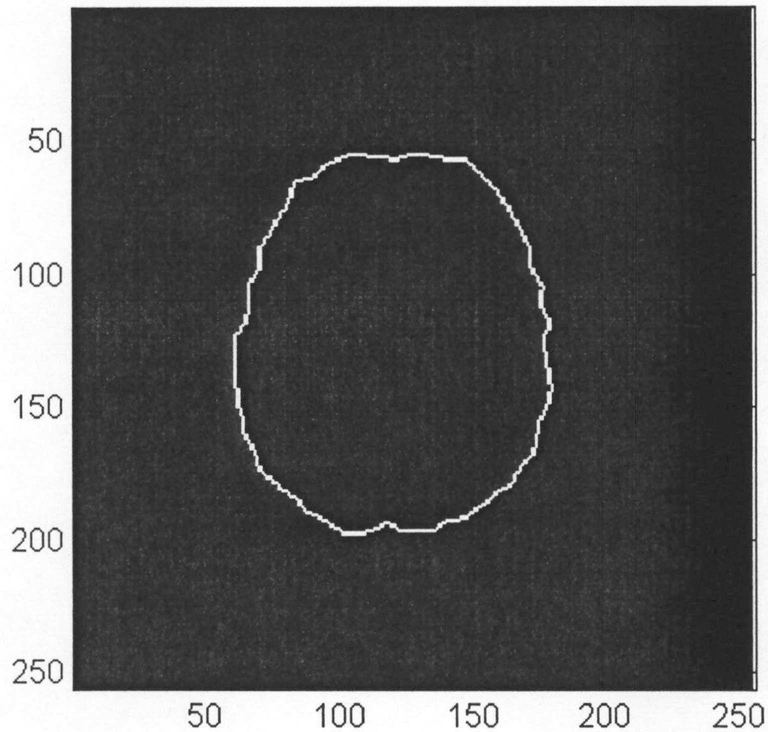

Figure 5.3. PET scan contour image [50].

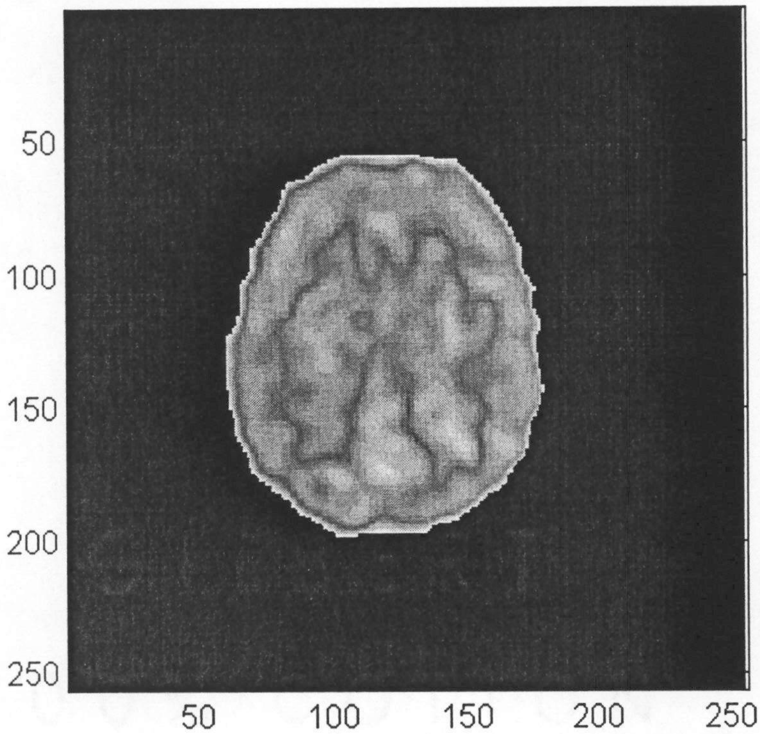

Figure 5.4. Resulting de-noised PET scan [50].

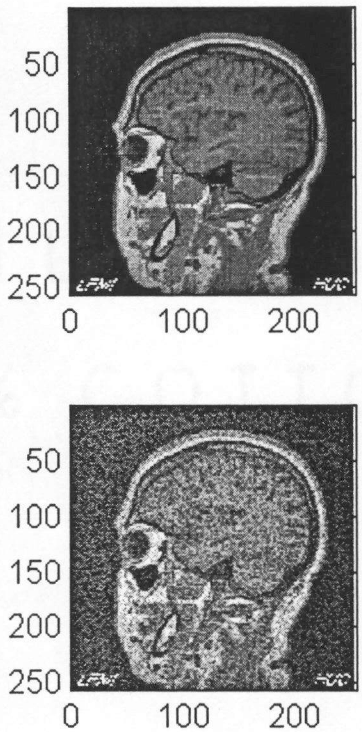

Figure 5.5. MRI image [52]. (a) original image, (b) noisy image.

depict an original sagittal MRI scan and its noisy representation obtained by the addition of random noise to the image. Results achieved by applying the wavelet transform with a Daubechies basis function (Daub2), decomposition level 3, and automatic threshold selection to the noisy image are conveyed in Figure 5.6a, while the corresponding 1-D representation of a specific row (row 120) of image results is displayed in Figure 5.7. It becomes therefore apparent that the wavelet transform does indeed adequately remove the noise from the image.

The wavelet packet representation of the noise removal procedure with a Daub2 basis function, SURE entropy parameter, decomposition level 3, and global threshold of 24 is also depicted in Figure 5.6b. Its 1-D representation is conveyed in Figure 5.7. As explained in Section 5.2.1, the SURE entropy parameter refers to a threshold selection rule based on Stein's Unbiased Risk Estimate (quadratic loss function) that may be utilized for denoising with the wavelet packet analysis [42,55]. One gets an estimate of the risk for a particular threshold value t. By minimizing the risks in t, a selection of the threshold value is obtained. The resulting data shows that the wavelet packet provides for a better noise removal than its wavelet counterpart. A larger number of bases being originated by a single decomposition introduces here more flexibility in the representation of the system, allowing for a more accurate characterization of the image with a few optimal dyadic coefficient blocks.

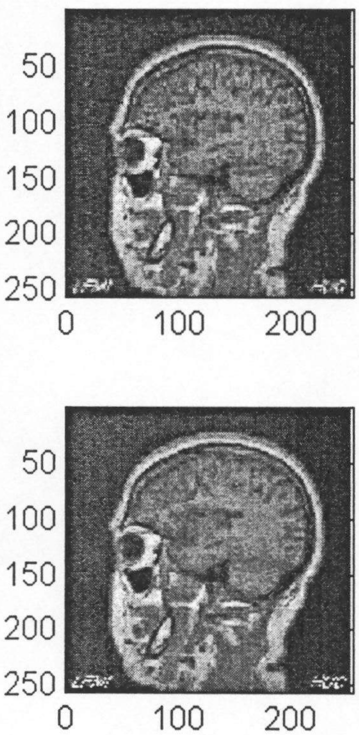

Figure 5.6. Denoised MRI image [52]. (a) denoising by wavelet framework,

(b) denoising by wavelet packet framework.

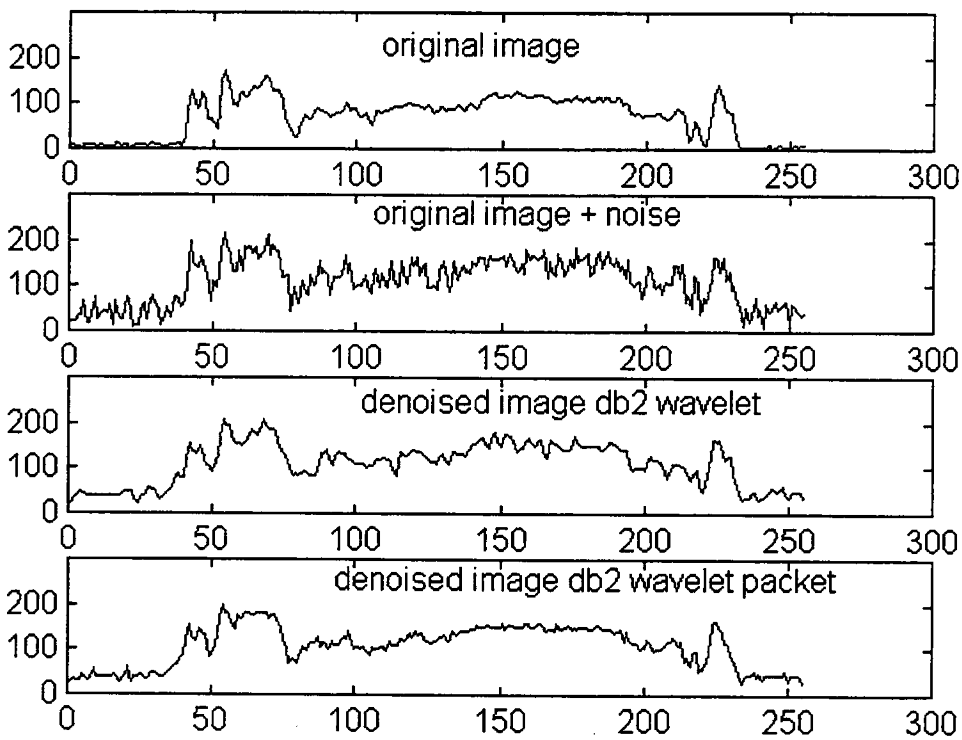

Figure 5.7. 1-D representation of the denoising process.

5.3.2 Contrast Enhancement

The improvement of the contrast in a medical image may often facilitate the visualization of specific features of interest and of details that may otherwise not be detected by an inspection of the original image. There are many methods in fields such as classical image processing, artificial intelligence, mathematical morphology, and digital filter theory that adequately perform image enhancement. This section only illustrates the application of one of the most popular digital filtering techniques in the improvement of image contrast, and introduces the wavelet transform as a powerful alternative procedure. Figure 5.8 depicts the result obtained by applying a 3 x 3 unsharp contrast enhancement filter to the PET scan in Figure 4.6. A wavelet transform with a Daubechies basis function (Daub2) and decomposition level 2 applied to the same image of Figure 4.6 produces the result shown in Figure 5.9. While the unsharp filter improves the contrast of all features in a globalized manner in Figure 5.8, the wavelet transform allows for a local enhancement of one or more features at a physician's criteria, as seen in Figure 5.9. This local enhancement is achieved by the manipulation of the wavelet coefficients of the feature at the level of resolution where the feature is best characterized.

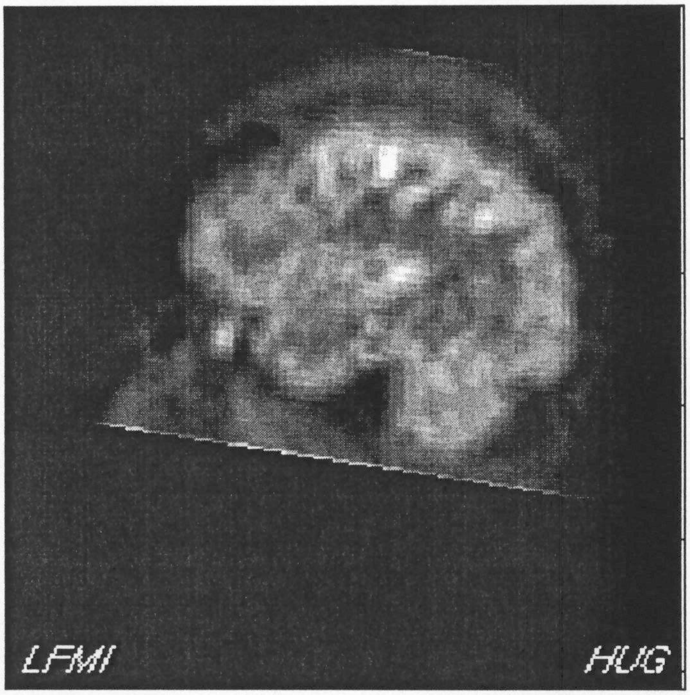

Figure 5.8. Unsharp filter applied to sagittal PET [52].

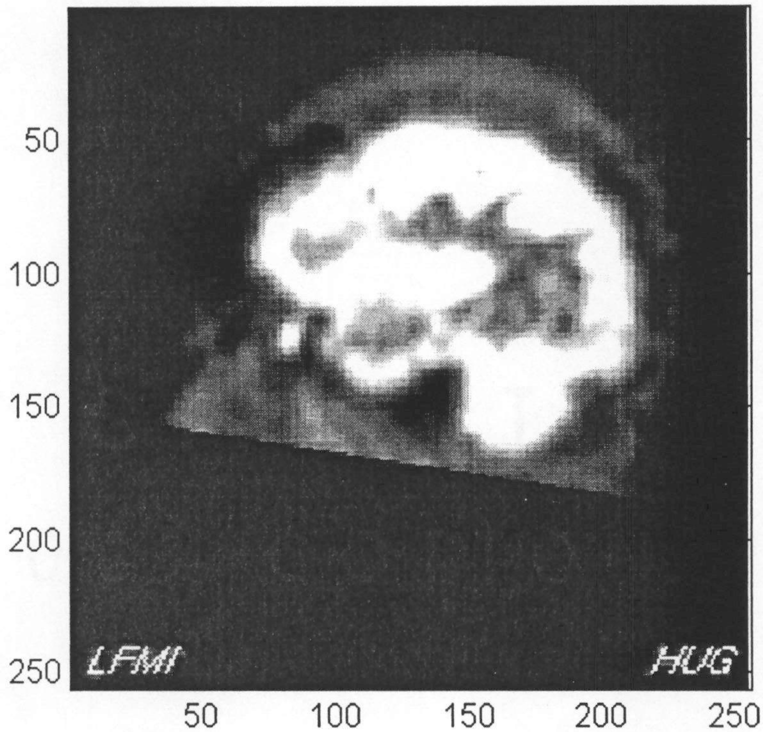

Figure 5.9. Wavelet enhancement of PET image [52].

CHAPTER 6

CONCLUSIONS AND RECOMMENDATIONS

6.1 Conclusions

The objective of this research was to develop an alternative methodology for the fusion of medical images of different modalities so as to facilitate faster and expedient medical diagnosis. The method described incorporates the strengths of wavelets and fuzzy logic in a hybrid system, whose merits have been clearly elucidated in the course of this thesis. Furthermore, the hybrid fuzzy-wavelet fusion scheme is completely implemented in MATLAB, a powerful, relatively simple, and versatile software that is supported in different computational environments, and easily transported across platforms.

The wavelet transform approach owes its popularity in the scientific world to its distinct capability of performing very good spatial resolution at high frequencies, as well as good frequency resolution at low frequencies. Since biomedical signals are most often of a nonstationary nature, wavelet transforms are specially suited for their analysis. As Akay [3] comments, " the wavelet method acts as a sort of mathematical microscope through which different parts of the signal may be examined by adjusting the focus." A wavelet packet transform analysis is introduced in this thesis as a powerful alternative for preprocessing tasks such as noise removal and contrast enhancement of medical images, and the results obtained prove the superiority of the technique as compared to some classical methods cited. The advantage in utilizing wavelets for noise removal lies in their ability to localize and selectively remove the problematic frequency components, portraying the relevant features of the image in a clear, uncorrupted manner. Likewise, an image feature of interest may be identified at a specific level of wavelet decomposition and locally enhanced by a chosen factor prior to image reconstruction. Classical techniques only allow a general globalized improvement of all features. In addition, the wavelet method provides the ability to reconstruct only chosen image components at certain decomposition levels, which facilitates a progressive study of a pathological condition such as a tumor in a sequential 2-D or 3-D image study.

An image fusion method [36] based on a wavelet transform analysis, labeled as "classical" in the present work, has been implemented in order to verify the suitability of the wavelet transform component of the proposed hybrid approach in the fusion of multimodality clinical images. This technique is superior to its Laplacian pyramid predecessor, since the fused output does not present blocking artifacts, which are common with the Laplacian pyramid fused result, when the images to be combined are very different. The results obtained with this wavelet fusion approach shown in Chapter 4 prove that anatomical and functional information from different images may be blended in a fused output in a versatile manner. This procedure presents the flexibility of being expanded and modified to support a variety of rules for the fusion of wavelet coefficients, which include operators defined on maximum and minimum values of coefficients, thresholds, multiplication and addition factors, and masks.

The second component introduced in this work in the development of the fuzzy-wavelet method for medical image fusion is the fuzzy inference system (FIS). Since feature boundaries and other image components are traditionally ill-defined in medical images due to many difficulties associated with the imaging of living organisms and hardware limitations, fuzzy logic proves to be well suited to the representation of data with such characteristics. The modeling of medical image data with a FIS permits a very flexible portrayal of the intrinsic gray-level structure and characteristics of an image through the association of membership functions of different shapes and numbers with inference rules specifically designed and adjusted for the intended task.

The integration of wavelets and fuzzy logic in the fuzzy-wavelet fusion scheme does, therefore, combine the advantages of both techniques in a single analytical tool. The preliminary analysis and initial system model developed in this work already evidence the impressive potential of the hybrid approach. The resulting images depict an excellent combination of the anatomical and functional information of registered scans. The system models the fusion process and rules with only three membership functions and nine inference rules, providing an evaluation tool that may be implemented by physicians for a quick-look capability during the process of diagnosis.

The fuzzy-wavelet fusion method also provides an additional feature of great significance: it allows for a simultaneous enhancement of image features without the need of threshold computations and other complex manipulations of wavelet coefficients as with the classical wavelet fusion technique. Finally, the greatest advantage of the hybrid scheme is that all relevant content and characteristic features of the input MRI and PET images may be fully represented in the output by fusing only the corresponding matrices of wavelet approximation coefficients at the chosen level of decomposition. This allows for noise removal, since the detail wavelet coefficients which characterize higher frequency components (noise) are not included in the actual fusion procedure. With the classical wavelet fusion method, on the other hand, all matrices of detail coefficients in addition to the matrix of approximation coefficients must be used for an adequate characterization of the fused output image. A detailed explanation and illustration of this observed particularity has been provided in Chapter 4. The fusion with the hybrid approach promotes, then, considerable savings in computational effort. A reduction in image storage space is also possible if the wavelet coefficients, instead of the image, are kept for a posterior reconstruction with the inverse wavelet transform.

In conclusion, it is important to emphasize that the performance evaluation of any technique dealing with the fusion of medical images requires in essence a subjective evaluation of results. A more detailed and systematic assessment of fusion results guided by the expert opinion of physicians would contribute to the optimization of the hybrid fuzzy-wavelet fusion technique and to the design of a metric for the evaluation of its effectiveness. Such ideas constitute recommendations for continuing research, which are provided in the following section.

6.2 Recommendations for Future Research

The potential of the hybrid fuzzy-wavelet technique for the fusion of medical images has been thoroughly exposed in its initial assessment in this work. An optimization of the system constitutes the next step in a future investigation, and the following suggestions are left for research:

- Perform a systematic and in-depth study of the many prototype wavelet functions in existence so as to identify potential candidates that describe the image and the nature of the problem being evaluated in an optimal manner;
- Search for an optimal combination of the fuzzy inference system parameters by experimenting with different shapes and numbers of membership functions, modifying inference parameters such as the implication and defuzzification functions, and verifying the feasibility and effect of introducing weighted inference rules in the design of the fusion system. The antecedents of the fuzzy rules might be assigned

different importances in terms of their contribution to the final decision, allowing the possibility of selection of certain image features of interest in the final fused output. This methodology would provide us with more insight on trends in the modeling and characterization of image features from different modalities of medical images with a fuzzy system;

- Submit results obtained with the fuzzy-wavelet fusion technique in this introductory feasibility study to radiologists and physicians for their comments relative to the performance of the hybrid fusion method, and for suggestions on improvements and further research of the applicability of the scheme;
- Create, with the help of the expert opinion of radiologists and physicians, a knowledge base for features to be identified in the fused image for specific pathological conditions, so as to optimize and tune the fuzzy-wavelet system to produce the desired results and aid a more reliable and accurate diagnosis of the conditions being evaluated;
- Develop a metric for the evaluation of the results obtained with the hybrid fusion system in order to validate the effectiveness of the technique;
- Apply different statistical techniques for the thresholding of wavelet coefficients in order to verify which method is better suited for the denoising of medical images;
- Investigate the modifications and improvements that would need to be introduced in the fuzzy-wavelet system to generalize its application to any set of medical images.

LIST OF REFERENCES

LIST OF REFERENCES

[1] P. A. Van den Elsen, E. D. Pol and M. A. Viergever, "Medical Image Matching - A Review with Classification," IEEE Engineering in Medicine and Biology, 11/12:26-39, March 1993.

[2] G. Q. Maguire Jr., M. E. Noz, et. al, "Graphics Applied to Medical Image Registration," IEEE Computer Graphics & Applications 20-28, March 1991.

[3] M. Akay, "Wavelet Applications in Medicine," IEEE Spectrum 50-56, May 1997.

[4] R. A. Hevenor and E. A. Margerum, "Edge Detection Using a Complex Wavelet," in Wavelet Applications, H. H. Szu Editor, Proc. SPIE 2242, pp. 888-896, 1994.

[5] D. J. Hebert, "A Fast-Wavelet Compass Edge Detector," in Wavelet Applications in Signal and Image Processing IV, Proc. SPIE 2825, pp. 432-442, 1996.

[6] T. E. Medl, "Innovative Uses of MATLAB Related to Medical Imaging and Image Analysis," http://www.mathwork.com/medl.html.

[7] R. C. Gonzalez and R. E. Woods, "Digital Image Processing," Reading, MS: Addison-Wesley Publishing Company, 1992.

[8] S. Mallat and W. L. Hwang, "Singularity Detection and Processing with Wavelets," IEEE Transactions on Information Theory, Vol. 38, No. 2, March 1992.

[9] S. Mallat and S. Zhong, "Characterization of Signals from Multiscale Edges," IEEE Transactions on Pattern Analysis and Machine Intelligence, Vol 14, No. 7, July 1992.

[10] J. Lu, J. B. Weaver, et. al, "Noise Reduction with a Multiscale Edge Representation and Perceptual Criteria," Proceeding of the IEEE-SP International Symposium on Time-Frequency and Time-Scale Analysis, Victoria, B.C., Canada, October 4-6, 1992.

[11] D. M. Healy Jr., J. Lu, and J. B. Weaver, "Two Applications of Wavelets and Related Techniques in Medical Imaging," Annals of Biomedical Engineering, Vol. 23, pp. 637-665, 1995.

[12] R. A. Carmona, W. L. Hwang and R. D. Frostig, "Wavelet Analysis for Brain-Function Imaging," University of California at Irvine, CA, May 4, 1994.

[13] J. Lu and D. M. Healy Jr., "Contrast Enhancement of Medical Images Using Multiscale Edge Representation," in Wavelet Applications, Proc. SPIE 2242, pp. 711-719, 1994.

[14] L. R. Myers Jr, C. M. Kocur, et.al, "Wavelets for Computer-Aided Breast Cancer Diagnosis," in Wavelet Applications II, Proc. SPIE 2491, part II, pp. 750-759, 1995.

[15] H. Yoshida, M. A. Anastasio, et. al, "Optimally Weighted Wavelet Packet Transform for Detection of Clustered Microcalcifications in Digital Mammograms," http://www.radonc.uchicago.edu/IWDM/IWDMa26.html.

[16] J. B. Weaver, D. M. Healy Jr., et. al, "Classification of Masses in Digitized Mammograms with Features in the Wavelet Transform Domain," in Wavelet Applications, Proc. SPIE 2242, pp. 704-710, 1994.

[17] B. B. Hubbard, "The World According to Wavelets," A. K. Peters Ltd., 1996.

[18] C. Kappeler and S. P. Müller, "Wavelet Compression of Noisy Tomographic Images," in Wavelet Applications in Signal and Image Processing III, Proc. SPIE 2569, pp. 644-652, 1995.

[19] A. F. Laine and X. Zong, "A Multiscale Sub-Octave Wavelet Transform for Denoising and Enhancement," Proc. SPIE 2825, pp. 238-249, 1996.

[20] E. D. Kolaczik, "Wavelet Shrinkage in Tomography," Proc. IEEE, pp. 1206-1207, June 1994.

[21] H. Szu, J. DeWitte, et. al, "Wavelet Transform for Local Tomography Reconstruction," in Wavelet Applications II, Proc. SPIE 2491, pp. 794-818, 1995.

[22] J. Olivo, J. Deubler and C. Boulin, "Automatic Registration of Images by a Wavelet-Based Multiresolution Approach," in Wavelet Applications in Signal and Image Processing III, Proc. SPIE 2569, pp. 234-244, 1995.

[23] C. H. Chen and G.G. Lee, "Multiresolution Wavelet Analysis Based Feature Extraction for Neural Network Classification," Proc. IEEE, pp. 1416-1421, 1996.

[24] P. Jensch, "Fusion of Fuzzy Type Image Modalities," in Medical Imaging VI, Proc. SPIE 1652, pp. 194-199, 1992.

[25] S. K. Pal and A. Rosenfeld, "Image Enhancement and Thresholding by Optimization of Fuzzy Compactness," Pattern Recognition Letters, Vol. 7, pp. 77-86, 1988.

[26] F. Russo and G. Ramponi, "A Totally Fuzzy Approach to Multisensor Instrumentation: Pre-Processing Techniques," Proc. IEEE, pp. 1143-1146, 1994.

[27] R. Acharya and N. Gai, "PET Reconstruction Using Multisensor Fusion Techniques," in Image Processing, Proc. SPIE 1445, pp. 207-221, 1991.

[28] P. F. Hemler, T. Sumanaweera, et.al, "A System for Multimodality Image Fusion," Proc. IEEE 7th. Symposium on Computer-Based Medical Systems, pp. 335-340, 1994.

[29] J. Owczarczyk, "Computer-Assisted Fusion of Multimodality Medical Images," Practical Aspects of Artificial Intelligence ICS PAS Publ., pp. 152-157, 1993.

[30] L. G. Brown, "A Survey of Image Registration Techniques, " ACM Computing Surveys, Vol. 24, No. 4, December 1992.

[31] A. Akerman III, "Pyramidal Techniques for Multisensor Fusion," in Fusion V, Proc. SPIE 1828, pp. 124-131, 1992.

[32] T. Ranchin, L. Wald and M. Mangolini, "Efficient Data Fusion Using Wavelet Transform: the Case of SPOT Satellite Images," in Mathematical Imaging, Proc. SPIE 2034, pp. 171-178, 1993.

[33] L. Graham and R. Adhami, "Fusion of Coincident Images Using Spatial Frequency Discrimination by Application of the Wavelet Transform, " Proc. IEEE, pp. 326-329, 1994.

[34] L. N. Graham, "Coincident Image Fusion Using the Discrete Wavelet Transform," M. Sc. Thesis, The University of Alabama in Huntsville, 1994.

[35] L. J. Chipman, T. M. Orr, and L. Graham, "Wavelets and Image Fusion," in Wavelet Applications in Signal and Image Processing III, Proc. SPIE 2569, pp. 208-219, 1995.

[36] H. Li, B. S. Manjunath and S. K. Mitra, "Multi-Sensor Image Fusion Using the Wavelet Transform," Proc. IEEE, pp. 51-55, 1994.

[37] E. V. Hoekstra, "Multiscale Analysis of Seismic Data by the Wavelet Transform," M. Sc. Thesis, Delft University of Technology, July 1996.

[38] I. Daubechies, "Ten Lectures on Wavelets, "Philadelphia, PA: Society for Industrial and Applied Mathematics, 1992.

[39] B. Vidakovic and P. Müller, "Wavelets for Kids," ftp://ftp.isds.duke.edu/pub/User/brani/papers/.

[40] A. Graps, "An Introduction to Wavelets," http://www.best.com/~agraps/agraps.html.

[41] G. Kaiser, "A Friendly Guide to Wavelets, "Birkhäuser, Boston, MA, 1994.

[42] M. Misiti, Y. Misiti, et. al, "Wavelet Toolbox," The MathWorks, Inc., Natick, MA, 1996.

[43] S. Mallat, "A Theory for Multiresolution Signal Decomposition: The Wavelet Representation, " IEEE Transaction on Pattern Analysis and Machine Intelligence, Vol. 11, No. 7, 674-693, July 1989.

[44] C. K. Chui, "An Introduction to Wavelets," Academic Press, Boston, MA, 1992.

[45] K. R. Castleman, "Digital Image Processing," Prentice-Hall, Inc., Englewood Cliffs, NJ, 1996.

[46] L. H. Tsoukalas and R. E. Uhrig, "Fuzzy and Neural Approaches in Engineering," John Wiley & Sons, Inc., New York, NY, 1997.

[47] N. Gulley and J.-S. R. Jang, "Fuzzy Logic Toolbox," The MathWorks, Inc., Natick, MA, 1995.

[48] R. Woods, "Automated Image Registration - AIR3.0," http://bishopw.loni.ucla.edu/AIR3/index.html.

[49] N. Ostu, "A Threshold Selection Method from Gray-Level Histograms," IEEE Transactions on Systems, Man, and Cybernetics, Vol. SMC-9, No. 1, January 1979.

[50] UTMC Department of Radiology, Personal Communication, University of Tennessee Medical Center at Knoxville, TN, USA, 1995.

[51] Harvard Medical School, "The Whole Brain Atlas," http://www.med.harvard.edu/AANLIB/home.html.

[52] Luc Bidaut, Personal Communication, Geneva University Hospitals, DIM - Radiology Department., Geneva, Switzerland, 1997.

[53] S. Webb, "The Physics of Medical Imaging," Philadelphia, PA: Institute of Physics Publishing, 1990.

[54] I. Alguíndigue and S. Smullen, "Segmenting MRI Images Using Self-Organizing Maps," Submitted for consideration to the International Conference on Computer Applications in Engineering and Medicine, Indianapolis, Indiana, March 15-17, 1995.

[55] C. Chiann and P. Morettin, "A Wavelet Analysis for Stationary Processes," http://www.ime.usp.br/~pam/.

[56] P. K. Sahoo, S. Soltani, et. al, "A Survey of Thresholding Techniques," Computer Vision, Graphics, and Image Processing, Vol. 41, pp. 233-260, 1988.

[57] D. L. Donoho, I. M. Johnstone, "Ideal Spatial Adaptation by Wavelet Shrinkage," Biometrika, Vol. 81, pp. 425-455, 1994.

[58] D. L. Donoho, "Nonlinear Wavelet Methods for Recovery of Signals, Densities, and Spectra from Indirect and Noisy Data," Proceedings of Symposia in Applied Mathematics, Vol. 47, pp. 173-205, 1993.

[59] D. L. Donoho, I. M. Johnstone, G. Kerkyacharian, D. Picard, "Wavelet Shrinkage: Asymptotia, " Journal of the Royal Statistics Society, series B, Vol. 57, No. 2, pp. 301-369, 1995.

APPENDIX

LISTING OF THE COMPUTER PROGRAMS

Program 1

```
load gaspet.img;
load gasmri.img;
load black;

[t,d]=wpdec2(gaspet,3,'bior3.7', 'shannon');
[t1,d1]=wpjoin(t,d,[2 3]);
[t2,d2]=wpjoin(t1,d1,[2 2]);
[t3,d3]=wpjoin(t2,d2,[2 1]);
[t4,d4]=wpjoin(t3,d3,[1 3]);
[t5,d5]=wpjoin(t4,d4,[1 2]);
[t6,d6]=wpjoin(t5,d5,[1 1]);

[k,l]=wpdec2(gasmri,3,'bior3.7', 'shannon');
[k1,l1]=wpjoin(k,l,[2 3]);
[k2,l2]=wpjoin(k1,l1,[2 2]);
[k3,l3]=wpjoin(k2,l2,[2 1]);
[k4,l4]=wpjoin(k3,l3,[1 3]);
[k5,l5]=wpjoin(k4,l4,[1 2]);
[k6,l6]=wpjoin(k5,l5,[1 1]);

[m,n]=wpdec2(black,3,'bior3.7', 'shannon');
[m1,n1]=wpjoin(m,n,[2 3]);
[m2,n2]=wpjoin(m1,n1,[2 2]);
[m3,n3]=wpjoin(m2,n2,[2 1]);
[m4,n4]=wpjoin(m3,n3,[1 3]);
[m5,n5]=wpjoin(m4,n4,[1 2]);
[m6,n6]=wpjoin(m5,n5,[1 1]);

c1=wdatamgr('read_cfs',d6,t6,[1,1]);
c2=wdatamgr('read_cfs',d6,t6,[1,2]);
c3=wdatamgr('read_cfs',d6,t6,[1,3]);
c4=wdatamgr('read_cfs',d6,t6,[2,1]);
c5=wdatamgr('read_cfs',d6,t6,[2,2]);
c6=wdatamgr('read_cfs',d6,t6,[2,3]);
c7=wdatamgr('read_cfs',d6,t6,[3,1]);
c8=wdatamgr('read_cfs',d6,t6,[3,2]);
```

```
c9=wdatamgr('read_cfs',d6,t6,[3,3]);
c10=wdatamgr('read_cfs',d6,t6,[3,0]);

c11=wdatamgr('read_cfs',l6,k6,[1,1]);
c12=wdatamgr('read_cfs',l6,k6,[1,2]);
c13=wdatamgr('read_cfs',l6,k6,[1,3]);
c14=wdatamgr('read_cfs',l6,k6,[2,1]);
c15=wdatamgr('read_cfs',l6,k6,[2,2]);
c16=wdatamgr('read_cfs',l6,k6,[2,3]);
c17=wdatamgr('read_cfs',l6,k6,[3,1]);
c18=wdatamgr('read_cfs',l6,k6,[3,2]);
c19=wdatamgr('read_cfs',l6,k6,[3,3]);
c20=wdatamgr('read_cfs',l6,k6,[3,0]);

new1=wdatamgr('read_cfs',n6,m6,[1,1]);
new2=wdatamgr('read_cfs',n6,m6,[1,2]);
new3=wdatamgr('read_cfs',n6,m6,[1,3]);
new4=wdatamgr('read_cfs',n6,m6,[2,1]);
new5=wdatamgr('read_cfs',n6,m6,[2,2]);
new6=wdatamgr('read_cfs',n6,m6,[2,3]);
new7=wdatamgr('read_cfs',n6,m6,[3,1]);
new8=wdatamgr('read_cfs',n6,m6,[3,2]);
new9=wdatamgr('read_cfs',n6,m6,[3,3]);
new10=wdatamgr('read_cfs',n6,m6,[3,0]);

%Combining level 1 details

for i=1:size(c1,1)
for j=1:size(c1,2)
 if abs(c1(i,j)) >= abs(c11(i,j))
    new1(i,j) = c1(i,j);
 else
    new1(i,j) = c11(i,j);
 end
end
end

for i=1:size(c2,1)
for j=1:size(c2,2)
 if abs(c2(i,j)) >= abs(c12(i,j))
    new2(i,j) = c2(i,j);
 else
    new2(i,j) = c12(i,j);
```

```
 end
end
end

for i=1:size(c3,1)
for j=1:size(c3,2)
 if abs(c3(i,j)) >= abs(c13(i,j))
     new3(i,j) = c3(i,j);
 else
     new3(i,j) = c13(i,j);
 end
end
end

% Combining level 2 details

for i=1:size(c4,1)
for j=1:size(c4,2)
 if abs(c4(i,j)) >= abs(c14(i,j))
     new4(i,j) = c4(i,j);
 else
     new4(i,j) = c14(i,j);
 end
end
end

for i=1:size(c5,1)
for j=1:size(c5,2)
 if abs(c5(i,j)) >= abs(c15(i,j))
     new5(i,j) = c5(i,j);
 else
     new5(i,j) = c15(i,j);
 end
end
end

for i=1:size(c6,1)
for j=1:size(c6,2)
 if abs(c6(i,j)) >= abs(c16(i,j))
     new6(i,j) = c6(i,j);
 else
     new6(i,j) = c16(i,j);
 end
```

```
end
end

%Combining level 3 details

for i=1:size(c7,1)
for j=1:size(c7,2)
 if abs(c7(i,j)) >= abs(c17(i,j))
    new7(i,j) = c7(i,j);
 else
    new7(i,j) = c17(i,j);
 end
end
end

for i=1:size(c8,1)
for j=1:size(c8,2)
 if abs(c8(i,j)) >= abs(c18(i,j))
    new8(i,j) = c8(i,j);
 else
    new8(i,j) = c18(i,j);
 end
end
end

for i=1:size(c9,1)
for j=1:size(c9,2)
 if abs(c9(i,j)) >= abs(c19(i,j))
    new9(i,j) = c9(i,j);
 else
    new9(i,j) = c19(i,j);
 end
end
end

% Combining level 3 approximation

for i=1:size(c10,1)
for j=1:size(c10,2)
 if abs(c10(i,j)) >= abs(c20(i,j))
    new10(i,j) = c10(i,j);
 else
    new10(i,j) = c20(i,j);
```

```
 end
end
end

% Writing new coefficients into "black" matrix

n6=wdatamgr('write_cfs',n6,m6,[1,1],new1);
n6=wdatamgr('write_cfs',n6,m6,[1,2],new2);
n6=wdatamgr('write_cfs',n6,m6,[1,3],new3);
n6=wdatamgr('write_cfs',n6,m6,[2,1],new4);
n6=wdatamgr('write_cfs',n6,m6,[2,2],new5);
n6=wdatamgr('write_cfs',n6,m6,[2,3],new6);
n6=wdatamgr('write_cfs',n6,m6,[3,1],new7);
n6=wdatamgr('write_cfs',n6,m6,[3,2],new8);
n6=wdatamgr('write_cfs',n6,m6,[3,3],new9);
n6=wdatamgr('write_cfs',n6,m6,[3,0],new10);

% Reconstruction - creating fused image

fused2 = wprec2(m6,n6);

% save fused1 fused1
```

Program 2

```
load pet60;
load mri60;
load black;

[t,d]=wpdec2(pet60,2,'bior3.7', 'shannon');
[t4,d4]=wpjoin(t,d,[1 3]);
[t5,d5]=wpjoin(t4,d4,[1 2]);
[t6,d6]=wpjoin(t5,d5,[1 1]);

[k,l]=wpdec2(mri60,2,'bior3.7', 'shannon');
[k4,l4]=wpjoin(k,l,[1 3]);
[k5,l5]=wpjoin(k4,l4,[1 2]);
[k6,l6]=wpjoin(k5,l5,[1 1]);

[m,n]=wpdec2(black,2,'bior3.7', 'shannon');
[m4,n4]=wpjoin(m,n,[1 3]);
[m5,n5]=wpjoin(m4,n4,[1 2]);
```

```
[m6,n6]=wpjoin(m5,n5,[1 1]);

c1=wdatamgr('read_cfs',d6,t6,[1,1]);
c2=wdatamgr('read_cfs',d6,t6,[1,2]);
c3=wdatamgr('read_cfs',d6,t6,[1,3]);
c4=wdatamgr('read_cfs',d6,t6,[2,1]);
c5=wdatamgr('read_cfs',d6,t6,[2,2]);
c6=wdatamgr('read_cfs',d6,t6,[2,3]);
c10=wdatamgr('read_cfs',d6,t6,[2,0]);

c11=wdatamgr('read_cfs',l6,k6,[1,1]);
c12=wdatamgr('read_cfs',l6,k6,[1,2]);
c13=wdatamgr('read_cfs',l6,k6,[1,3]);
c14=wdatamgr('read_cfs',l6,k6,[2,1]);
c15=wdatamgr('read_cfs',l6,k6,[2,2]);
c16=wdatamgr('read_cfs',l6,k6,[2,3]);
c20=wdatamgr('read_cfs',l6,k6,[2,0]);

new1=wdatamgr('read_cfs',n6,m6,[1,1]);
new2=wdatamgr('read_cfs',n6,m6,[1,2]);
new3=wdatamgr('read_cfs',n6,m6,[1,3]);
new4=wdatamgr('read_cfs',n6,m6,[2,1]);
new5=wdatamgr('read_cfs',n6,m6,[2,2]);
new6=wdatamgr('read_cfs',n6,m6,[2,3]);
new10=wdatamgr('read_cfs',n6,m6,[2,0]);

%Combining level 3 approximations

q19= max(max(abs(c10)));
q20= max(max(abs(c20)));
rat = q20/q19;
for i=1:size(c10,1)
for j=1:size(c10,2)
    c10(i,j) = rat*c10(i,j);
end
end
fuzf=readfis('fus11a.fis');

for i=1:size(c10,1)
for j=1:size(c10,2)
   x1=c10(i,j);
   x2=c20(i,j);
y=evalfis([x1 x2],fuzf);
```

```
new10(i,j)=y;
end
end
clear fuzf;

% Writing new coefficients into "black" matrix

l6=wdatamgr('write_cfs',l6,k6,[2,0],new10);

% Reconstruction - creating fused image

biorson= wprec2(k6,l6);

% save biorson biorson
```

Fuzzy Inference System

1. Name FUS11A
2. Type mamdani
3. Inputs/Outputs [2 1]
4. NumInputMFs [3 3]
5. NumOutputMFs 3
6. NumRules 9
7. AndMethod min
8. OrMethod max
9. ImpMethod min
10. AggMethod max
11. DefuzzMethod centroid
12. InLabels x1

13. x2

14. OutLabels y

15. InRange [-1745 1745]

16. [-1745 1745]

17. OutRange [-1745 1745]

18. InMFLabels SM

19. MN

20. MP

21. SM

22. MN

23. MP

24. OutMFLabels SM

25. MN

26. MP

27. InMFTypes trimf

28. trimf

29. trimf

30. trimf

31. trimf

32. trimf

33. OutMFTypes trimf

34. trimf

35. trimf

36. InMFParams [-669.1 0 669.1 0]

37. [-1745 -921.3 -291.2 0]

38. [290.6 921.3 1745 0]

39. [-669.1 0 669.1 0]

40. [-1745 -921.3 -291.2 0]

41. [290.6 921.3 1745 0]

42. OutMFParams [-669.1 0 669.1 0]

43. [-1745 -921.3 -291.2 0]

44. [290.6 921.3 1745 0]

45. RuleList [2 2 2 1 1]

46. [2 1 2 1 1]

47. [2 3 3 1 1]

48. [1 2 2 1 1]

49. [1 1 1 1 1]

50. [1 3 3 1 1]

51. [3 2 3 1 1]

52. [3 1 3 1 1]

53. [3 3 3 1 1]

Program 3

```
# include <stdio.h>
# include <math.h>

void Read_image(void);
void Threshold(void);
void Write_image(void);

int row, column;
int i, j, k, nbits, levels, grlev, size, wd, ht, nr, nc;
int image[256][256], newimg[256][256], tres;
char h1[10];

void main(void){

  Read_image();
  Threshold();
  Write_image();
}

void Read_image(void){

 size=256;
  wd=size; ht=size;
  scanf("%s", &h1);
  scanf("%i %i", &nr, &nc);
  scanf("%i", &levels);
  for(i = 0; i < size; i++){
    for(j =0; j < size; j++){
      scanf("%d", &image[i][j]);
    }
  }

}

void Threshold(void){
  double pi[256], sigma_T= 0.0, mu_t[256], sigma_B[256], w0[256];
  double w1[256], mu_1[256], mu_0[256], mu_T=0.0;
  int ni[256], g, gray_levels = 256, n;
  double t[256];
  double temp, max;
  int index;
  n = size * size;
  for(i=0;i<gray_levels;i++){
```

```
        ni[i] = 0;
        mu_t[i] = 0.0;
        w0[i] = 0.0;
}
        /* calculating the frequencies */

  for(i= 0; i < size; i++)
            {       for(j= 0; j < size; j++)
                    {     g = image[i][j];
                            ni[g]++;
                    }
            }
 /* calculating the probabilities */

 for(i=0; i<gray_levels; i++)
        {pi[i] = (double) ni[i]/n ;}

/* calculating the total variance */
        for(i=0; i< gray_levels;i++)
                mu_T = mu_T + (double) (i * pi[i]);
        for(i=0; i < gray_levels; i++)
        {       temp = (double) (i - mu_T);
                temp = temp * temp;
                sigma_T = sigma_T + (temp * pi[i]);
        }

/* calculate the other variances (one per pixel) */
for(i=0; i<gray_levels; i++)
{   for(j=0; j<=i; j++)
        {       w0[i] = w0[i] + pi[j];
                mu_t[i] = mu_t[i] + (double) (j * pi[j]);
        }
        w1[i] = 1.0 - w0[i];
        mu_0[i] = mu_t[i] / w0[i];
        if(w1[i] == 0.0) mu_1[i] = 2000.0;
        else
                mu_1[i] = (mu_T - mu_t[i])/w1[i];

        temp = (mu_1[i] - mu_0[i]);
        temp =  temp * temp;
        sigma_B[i] = w0[i]*w1[i];
        sigma_B[i] =(sigma_B[i] * temp);
}
```

```
  max=-100.0;
  for(i=0;i<gray_levels;i++)
        {
        t[i] = sigma_B[i] / sigma_T;
     if(t[i]>max){
      index=i;
      max=t[i];
     }
  }

  tres=index;

  for(i= 0; i < size; i++){
    for(j= 0; j < size; j++){
         if(image[i][j] <= tres)
             newimg[i][j]=0;
         if(image[i][j] > tres)
             newimg[i][j]=image[i][j];

    }
  }
}
void Write_image(void){
 printf("P2\n");
  printf(" 256 256\n");
  printf("255\n");
  for(i = 0; i <size; i++){
   for(j = 0; j < size; j++){
    printf("%d ", newimg[i][j]);
   }
   printf("\n");
  }
}
```

Program 4

```
#include <stdio.h>
#include <math.h>

#define size 256
#define white 1
#define black 0
```

```
void Read_image(void);
void Outline(void);
void Write_image(void);

int row, column, wd, ht, nr, nc, levels;
int i, j, k;
int image[size][size], newimg[size][size], whiteimg[size][size], novaimg[size][size];
char h1[10];
FILE *myfile1;
FILE *myfile2;
void main(void)
{
 myfile1 = fopen("f20os.img", "r");
 myfile2 = fopen("f20headb.img", "w");

 Read_image();
 fclose(myfile1);
 Outline();
 Write_image();

}
void Read_image(void)
{
 double temp;
 wd=size; ht=size;
 fscanf(myfile1, "%s", &h1);
 fscanf(myfile1, "%i %i", &nr, &nc);
 fscanf(myfile1,"%i", &levels);
 for(i = 0; i < size; i++){
  for(j =0; j < size; j++){
   fscanf(myfile1, "%d", &image[i][j]);
      newimg[i][j] = black;
   }
 }
}

void Outline(void)
{
int i, j, k, l;
int pixel;

for(i=0; i<size; i++){
        for(j=0; j<256; j++)
```

```
                if(image[i][j] != black)
                {       newimg[i][j] = white;
                        break;
            }
      for(j=255; j>=0; j--)
                if(image[i][j] != black)
                {       newimg[i][j] = white;
                        break;
            }
}
for(j=0; j<size; j++){
        for(i=0; i<256; i++)
                if(image[i][j] != black)
                {       newimg[i][j] = white;
                        break;
            }
      for(i=255; i>=0; i--)
                if(image[i][j] != black)
                {       newimg[i][j] = white;
                        break;
            }
}
}
void Write_image(void)
{
 fprintf(myfile2,"P2\n");
  fprintf(myfile2," 256 256\n");
  fprintf(myfile2,"255\n");
  for(i = 0; i <size; i++){
    for(j = 0; j < size; j++){
      fprintf(myfile2,"%d ", newimg[i][j]);
    }
    fprintf(myfile2,"\n");
  }
fclose(myfile2);
}
```

Program 5

```
#include <stdio.h>
#include <math.h>
```

```
#define size 256
#define white 1
#define black 0
void Read_image(void);
void Finalproc(void);
void Write_image(void);

int row, column, wd, ht, nr, nc, levels;
int i, j, k;
int image[size][size], newimg[size][size], imageold[size][size], imageold2[size][size];
char h1[10];
FILE *myfile1;
FILE *myfile2;
FILE *myfile3;
void main(void)
{
 myfile1 = fopen("f20headb.img", "r");
 myfile3 = fopen("f20or.img", "r");
 myfile2 = fopen("f20fin.img", "w");
 Read_image();
 fclose(myfile1);
 fclose(myfile3);
 Finalproc();
 Write_image();

}
void Read_image(void)
{
 wd=size; ht=size;
 fscanf(myfile1, "%s", &h1);
 fscanf(myfile1, "%i %i", &nr, &nc);
 fscanf(myfile1,"%i", &levels);
 fscanf(myfile3, "%s", &h1);
 fscanf(myfile3, "%i %i", &nr, &nc);
 fscanf(myfile3,"%i", &levels);

 for(i = 0; i < size; i++){
  for(j =0; j < size; j++){
    fscanf(myfile1, "%d", &image[i][j]);
    fscanf(myfile3, "%d", &imageold[i][j]);
    }
 }
}
```

```
void Finalproc(void)
{
int i, j, k,y,h;
int pixel;
double temp = 0.0;
int t=0;
for(i=0; i<size; i++){
        t= 0;
        for(j=0; j<256; j++){

if(image[i][j] != 0)
{
        for ( k=255;k>j;k--)
                {
    if(image[i][k] != 0)
          {
                t=k;
                k=j;

          }
         }
        for( y=j; y<t;y++)
                newimg[i][y]=imageold[i][y];
                for(h=t; h<256;h++)
                {
                newimg[i][h]=0;
                }
j=256;
}else
newimg[i][j]=0;

        }
}
}
void Write_image(void)
{
 fprintf(myfile2,"P2\n");
  fprintf(myfile2," 256 256\n");
  fprintf(myfile2,"255\n");
  for(i = 0; i <size; i++){
    for(j = 0; j < size; j++){
      fprintf(myfile2,"%d ", newimg[i][j]);
```

```
    }
    fprintf(myfile2,"\n");
  }
fclose(myfile2);
}
```

Program 6

```
load gaspet.img;

[t,d]=wpdec2(gaspet,2,'db2', 'shannon');
%plottree(t); title('WP Decomposition Tree - Level 2 ');
%[at,ad]=wpjoin(t,d,[2 3]);
%[bt,bd]=wpjoin(at,ad,[2 2]);
%[ct,cd]=wpjoin(bt,bd,[2 1]);
[dt,dd]=wpjoin(t,d,[1 3]);
[et,ed]=wpjoin(dt,dd,[1 2]);
[ft,fd]=wpjoin(et,ed,[1 1]);
%plottree (ft);title('WP Wavelet Decomposition Tree - Level 2');
% print -dbitmap ft;

c1=wdatamgr('read_cfs',fd,ft,[1,1]);
c2=wdatamgr('read_cfs',fd,ft,[1,2]);
c3=wdatamgr('read_cfs',fd,ft,[1,3]);
c4=wdatamgr('read_cfs',fd,ft,[2,1]);
c5=wdatamgr('read_cfs',fd,ft,[2,2]);
c6=wdatamgr('read_cfs',fd,ft,[2,3]);
c10=wdatamgr('read_cfs',fd,ft,[2,0]);

% manipulating the data

% read and manipulate packet (1,1) coefficients
c1=wdatamgr('read_cfs',fd,ft,[1,1]);
a=max(max(abs(c1)));
for i=1:size(c1,1)
for j=1:size(c1,2)
  nc1(i,j) = 1*(c1(i,j));
end
end
fd=wdatamgr('write_cfs',fd,ft,[1,1],nc1);

% read and manipulate packet (1,2) coefficients
c2=wdatamgr('read_cfs',fd,ft,[1,2]);
```

```
b=max(max(abs(c2)));
for i=1:size(c2,1)
for j=1:size(c2,2)
  nc2(i,j) = 1*(c2(i,j));
end
end
fd=wdatamgr('write_cfs',fd,ft,[1,2],nc2);

% read and manipulate packet (1,3) coefficients
c3=wdatamgr('read_cfs',fd,ft,[1,3]);
q=max(max(abs(c3)));
for i=1:size(c3,1)
for j=1:size(c3,2)
  nc3(i,j) = 1*c3(i,j);
end
end
fd=wdatamgr('write_cfs',fd,ft,[1,3],nc3);

% read and manipulate packet (2,1) coefficients
c4=wdatamgr('read_cfs',fd,ft,[2,1]);
e=max(max(abs(c4)));
for i=1:size(c4,1)
for j=1:size(c4,2)
  nc4(i,j) = 1*(c4(i,j));
end
end
fd=wdatamgr('write_cfs',fd,ft,[2,1],nc4);

% read and manipulate packet (2,2) coefficients
c5=wdatamgr('read_cfs',fd,ft,[2,2]);
f=max(max(abs(c5)));
for i=1:size(c5,1)
for j=1:size(c5,2)
  nc5(i,j) = 1*(c5(i,j));
end
end
nfd=wdatamgr('write_cfs',fd,ft,[2,2],nc5);

% read and manipulate packet (2,3) coefficients
c6=wdatamgr('read_cfs',fd,ft,[2,3]);
g=max(max(abs(c6)));
for i=1:size(c6,1)
for j=1:size(c6,2)
```

```
  nc6(i,j) = 1*c6(i,j);
 end
end
fd=wdatamgr('write_cfs',fd,ft,[2,3],nc6);

% read and manipulate packet (2,0) coefficients
 c10=wdatamgr('read_cfs',fd,ft,[2,0]);
d=max(max(abs(c10)));
for i=1:size(c10,1)
  for j=1:size(c10,2)
     nc10(i,j) = 2.*c10(i,j);
  end
end
fd=wdatamgr('write_cfs',fd,ft,[2,0],nc10);

% reconstructing the image

gaspeteb= wprec2(ft,fd);
```

VITA

Marcia Kohls was born in Santa Cruz do Sul, RS, Brasil on November 14, 1969. She attended the Engineering Science and Mechanics Department at the University of Tennessee at Knoxville, TN, USA and received her B.S. degree in December 1992. From 1993 until 1996, she worked as a graduate teaching assistant at the Engineering Science and Mechanics Department. In 1997, she was granted an assistantship at the UT Energy, Environment, and Resources Center, and served as a student PC consultant. She received her Master of Science degree in August 1997, with a Minor in Statistics, and is currently employed as an engineer at Raytheon E-Systems in Dallas, TX.